

107  
/OPTIMIZATION OF SURGE IRRIGATION/

by

Terry William Ortel

B.S., Purdue University; 1984

---

A MASTER'S THESIS

submitted in partial fulfillment of the

requirements for the degree

MASTER OF SCIENCE

in

AGRICULTURAL ENGINEERING

Department of Agricultural Engineering

Kansas State University  
Manhattan, Kansas

1986

Approved by:

*Harry L. Manges*  
Major Professor

LD  
2668  
ST4  
1986  
077  
C. 2

TABLE OF CONTENTS

A11202 965126

	Page
ACKNOWLEDGEMENTS.....	1
LIST OF FIGURES.....	iii
LIST OF TABLES.....	v
INTRODUCTION.....	1
LITERATURE REVIEW.....	3
Field Evaluations.....	3
Irrigation Mathematical Models.....	5
Kinematic-Wave Approximation.....	8
Infiltration Models.....	9
Numerical Solution Technique.....	15
INVESTIGATIONS.....	23
Objectives.....	23
Field Studies.....	23
Results of Field Studies.....	29
Simulation Studies.....	36
Results of Simulation Studies.....	44
DISCUSSION.....	61
CONCLUSIONS.....	65
SUMMARY.....	66
SUGGESTIONS FOR FUTURE RESEARCH.....	68
REFERENCES.....	69
APPENDIX A.....	71
APPENDIX B.....	83

## ACKNOWLEDGEMENTS

Sincere thanks are given to Junior Leonard and Frank Phief for their cooperation in allowing surge tests to be performed on their irrigated fields. For their help in conducting the field work for this study, thanks are also given to Marvin Cronin Jr., Mike Lasch, Ramon Servantez, and Cheryl Timm. Thanks are extended to Pam Meyer for her help in typing this thesis. For the funding of this project, deep appreciation is given to the Agricultural Experiment Station. Appreciation is also extended to my parents for their financial and moral support.

Thanks are due to Dr. Bruce McEnroe for his advice and service on my graduate committee. Thanks are also due to Dr. Mark Hooker for his service on my graduate committee and his help in setting up and conducting the field experiments. Finally, deep appreciation is given to Dr. Harry Manges for his service as my major professor and advisor. Thanks are also due for his seemingly endless hours of help in the field and guidance in the resulting analysis.

## LIST OF FIGURES

	Page
Figure 1. Furrow Longitudinal Section Showing Wetted Perimeter Differences Occurring Between Surges.....	12
Figure 2. Clemmens Branch Infiltration Fuction.....	14
Figure 3. Computational Cell for Kinematic-Wave Model.....	16
Figure 4. Time-Space Computational Grid.....	19
Figure 5. Kinematic-Wave Simulation of Continuous Flow Advance and Recession.....	21
Figure 6. Kinematic-Wave Simulation of Surge Flow Advance and Recession.....	22
Figure 7. Dry, Rough Furrow Section.....	27
Figure 8. Previously Wetted, Smooth Furrow Section.....	27
Figure 9. Advance Rate Acceleration Over a Previously Wetted Furrow Section Observed During Surge Flow.....	30
Figure 10. Advance Rate Variations Observed for Two Adjacent Compacted Furrows During Continuous Flow.....	32
Figure 11. Advance Rate Variations Observed for Two Adjacent Compacted Furrows During Surge Flow.....	33
Figure 12. Reduction in Infiltrated Volume During Advance Under Surge Flow Resulting From a Step Drop to the Basic Rate After the Initial Wetting.....	40
Figure 13. Reduction in Infiltrated Volume During Advance Under Surge Flow Resulting From the Effects of Cumulative On- and Off-Times.....	43
Figure 14. Kinematic-Wave Simulation of Surge Flow Advance Assuming a Variable-Slope Profile and Surface Roughness.....	45
Figure 15. Kinematic-Wave Simulation of Surge Flow Advance Assuming a Variable-Slope Profile and Surface Roughness.....	46
Figure 16. Kinematic-Wave Simulation of Surge Flow Advance Assuming a Constant-Slope Profile and Surface Roughness.....	48
Figure 17. Kinematic-Wave Simulation of Surge Flow Advance Assuming a Constant-Slope Profile and Surface Roughness.....	50

Figure 18.	Model Simulation of Predicted Surge Flow Advance for 30-Minute Surge On-Times.....	51
Figure 19.	Model Simulation of Predicted Surge Flow Advance for 60-Minute Surge On-Times.....	52
Figure 20.	Model Simulation of Predicted Surge Flow Advance for 120-Minute Surge On-Times.....	53
Figure 21.	Model Simulation of Predicted Advance for Continuous Flow.....	54
Figure 22.	Model Simulation of Surge Flow Advance Using the SCS Design Equation With a 0.3 in/hr Intake Family.....	57
Figure 23.	Model Simulation of Surge Flow Advance Using the Clemmens Branch Infiltration Equation.....	59
Figure 24.	Model Simulation of Surge Flow Advance Using the SCS Design Equation With a 0.3 in/hr Intake Family.....	60

## LIST OF TABLES

	Page
Table 1. Total On-Time for Advance Completion During the First Irrigation at the Holcomb Experiment Field.....	35
Table 2. Total On-Time for Advance Completion During the Second Irrigation at the Holcomb Experiment Field.....	35
Table 3. Furrow Inflow Rates.....	72
Table 4. Surge Flow On-Times for Variable Cycle Times.....	73
Table 5. Pre-Irrigation Advance Times for Variable Surge On-Times at the Junior Leonard Site.....	74
Table 6. Advance Distances for Continuous Flow at the Holcomb Experiment Field.....	75
Table 7. Total Cumulative On-Times for Advance Completion at the Holcomb Experiment Field.....	76
Table 8. Pre-Irrigation Advance Distances for Continuous Flow at the Frank Phief Site.....	77
Table 9. Pre-Irrigation Advance Times Observed for the North Row at the Frank Phief Site.....	78
Table 10. Pre-Irrigation Advance Times Observed for the South Row at the Frank Phief Site.....	79
Table 11. First Irrigation Advance Times Observed for the North Row at the Frank Phief Site.....	80
Table 12. First Irrigation Advance Times Observed for the South Row at the Frank Phief Site.....	81
Table 13. Field Elevations at the Frank Phief Site.....	82

## INTROOUCION

Oeclining ground water tables in the Ogallala aquifer are causing increas-  
ing concern for the irrigators of western Kansas. This ground water table  
decline , combined with the rising costs of pumping water, results in a need to  
use water more efficiently.

In western Kansas there are two primary systems used to irrigate a crop.  
These are sprinkler systems and surface systems. Sprinkler irrigation is gen-  
erally an efficient way to apply water, although initial costs and energy costs  
are usually higher than for the surface system. Surface irrigation can be, but  
often times is not, an efficient method of applying water. Due to the rela-  
tively low efficiencies achieved by some current methods of surface irrigation,  
researchers need to find more efficient methods or techniques. Two such tech-  
niques are cutback flow and surge flow.

Cutback irrigation is the practice of reducing inflow into a field after  
advance is completed. The inflow is reduced or "cutback" to decrease the runoff  
from the end of the field. Ideally, the inflow is reduced to some optimum value  
for the given field conditions.

Surge irrigation is defined as the intermittent application of water to a  
furrow. Ouring surge irrigation, the inflow into the furrow is cycled on and  
off until the irrigation is completed. The duration of an individual on or off  
time can vary from a few minutes to several hours. The ratio of on time to off  
time is known as the cycle ratio.

Surge irrigation was originally conceived as a means of achieving cutback  
irrigation. The inflow would be surged on and off to produce a lower time

averaged value of inflow. Upon implementing surge irrigation, Bishop et al. (1981) found that for a given volume of water, the water advanced further down the field in the surge plots than in the continuous flow plots. Work conducted by other researchers supported this finding (Coolidge et al., 1982, Podmore et al., 1983, and Izuno, 1984). The benefit of using surge irrigation becomes apparent during the second and subsequent surge cycles. As the water advances in a previously wetted section of the furrow, the advance rate accelerates partially due to a reduction in the infiltration rate.

The lower infiltration rate, with subsequent faster advance rate, presents both potential benefits and harm to the irrigator. The benefit is a faster advance and more uniform application of water. The harm may occur after the completion of advance. Due to the lower infiltration rates, if surging is continued there exists the possibility that large runoff volumes will be produced. In surge irrigation, more so than in continuous irrigation, proper management appears to be the key.

One method of studying various management techniques is to conduct field experiments. The different strategies would be performed and evaluated according to crop yields, advance rate, uniformity of irrigation, and volume of water applied. This method yields reliable results, but is extremely labor intensive and, due to climatic reasons, cannot be conducted year round.

Another method of studying the effects of various management techniques is through computer simulation. In the current study, a kinematic wave model is updated and employed to evaluate the effects of various surge strategies.

## LITERATURE REVIEW

Surge irrigation is a relatively new strategy of surface irrigation. During surge irrigation, the inflow into the furrow is cycled on and off in increments of constant or variable time span. The time period required for one on/off cycle has been termed the cycle time. The cycle ratio is defined as the ratio of off time to on time.

## Field Evaluations

Surge flow was originally conceived as a means of automating cutback irrigation. Stringham and Keller (1979) reported, after their initial field studies, that the experimental surge flows produced a marked impact on the furrow advance rates. Likewise, Coolidge et al. (1982) and Izuno (1984) reported a significant acceleration in the advance rate for surge flow when compared to continuous flow. Bishop et al. (1981) and Podmore et al. (1983) found that surge flow required less water to complete advance than did continuous flow. Coolidge et al. (1982) reported that surge flow reduced the advance rate differences commonly found between compacted and noncompacted furrows (wheel traffic versus no wheel traffic). Using surge flow, Coolidge et al. (1982) and Izuno (1984) found that the seasonal variations in the water advance rate were reduced. Additionally, Izuno (1984) found that the advance rate of the third irrigation under continuous flow approached the advance rate found in irrigations one, two, and three under surge flow. The accelerated advance rate of surge flow was found to be a noncumulative process, tending to suggest that some upper limit of advance acceleration exists (Izuno, 1984).

Izuno (1984) reported that the effects of surge flow are less pronounced on tighter soils or under compacted conditions. Manges and Hooker (1984)

found that 60 minute surge times did not produce a significant increase in advance rate on a fine textured soil which cracked upon drying. A 120 minute surge on-time, however, was found to significantly reduce advance time for trafficked furrows during the third irrigation on this same soil (Manges and Hooker, 1984). Coolidge et al. (1982) reported that a relationship exists between the cycle on-time and the furthest advance distance possible. The 10 and 20 minute on-times were found to be a significant improvement over continuous flow, however, 5 minute on-times were not (Coolidge et al., 1982). Podmore et al. (1983) reported that the surge effect (faster advance) is less pronounced when the off-time between surges is insufficient to allow the free water to completely infiltrate.

Several researchers (Bishop et al., 1981, Podmore et al., 1983, and Izuno, 1984) have reported that there is a lower infiltration rate during surge flow. The accelerated advance rate observed in the field is at least partially due to this lowered infiltration rate. Theories for the infiltration reduction, as given in Izuno (1984), are outlined below:

1. surface sealing occurring on the soil surface due to the reorientation of the soil particles,
2. compaction of soil surface due to tension forces in the soil following drainage,
3. air entrapment within the pores of the soil matrix,
4. hydraulic gradient reduction due to infiltration and redistribution of water during previous surge cycles, and

5. hysteresis effects in the soil due to the wetting and drainage periods.

The lowered infiltration rate was found to benefit advance; however, upon advance completion, it has been found that large runoff volumes will be generated if surging is continued at the same flowrate and cycle times. Izuno and Podmore (1984) reported that continued surging at the same flowrate and cycle time after advance completion resulted in lower application efficiencies when compared to continuous flow. They compared similar total water application volumes between the surge flow tests and the continuous flow tests and found that the surge tests generated larger runoff volumes. Coolidge et al. (1982) reported that peak runoff rates were higher for surge flow than for continuous flow. Bassett et al. (1983) and Izuno and Podmore (1984) both found that surging until advance completion followed by cutback continuous flow resulted in the most optimum irrigation strategy. Bassett et al. (1983) and Izuno and Podmore (1984) warn of overgeneralizing their findings to cover all irrigation situations.

More likely than not, all of the aforementioned researchers would agree that additional studies need to be conducted using surge and cutback flows. Field studies are a reliable means to obtain results on the performance of an irrigation; however, a limited number of studies can be conducted per year. With the advent of the high speed computer, mathematical simulations of an irrigation strategy offer a fast and efficient means of evaluation. The development of the current mathematical models capable of simulating an irrigation event follows.

#### Irrigation Mathematical Models

Elliot et al. (1983a) classified flow in a furrow to be both unsteady and gradually varied. Two properties which must be satisfied by this type of flow are conservation of mass and conservation of momentum. The partial differential equation of mass conservation is:

$$\frac{\partial Q}{\partial x} + \frac{\partial A}{\partial t} + \frac{\partial Z}{\partial t} = 0 \quad [1]$$

The partial differential equation of motion is:

$$\frac{1}{g} \frac{\partial V}{\partial t} + \frac{V}{g} \frac{\partial V}{\partial x} + \frac{\partial y}{\partial x} = S_o - S_f + \frac{DIV}{gA} \quad [2]$$

In the above equations,  $Q$  is flowrate ( $L^3 T^{-1}$ ),  $x$  is distance from the head of the field ( $L$ ),  $A$  is cross-sectional flow area ( $L^2$ ),  $t$  is time ( $T$ ),  $Z$  is cumulative infiltration per unit area ( $L$ ),  $g$  is gravitational acceleration ( $LT^{-2}$ ),  $V$  is average velocity ( $LT^{-1}$ ),  $y$  is flow depth ( $L$ ),  $S_o$  is channel bottom slope ( $LL^{-1}$ ),  $S_f$  is friction slope ( $LL^{-1}$ ),  $D$  is a numerical constant, and  $I$  is volume rate of infiltration per unit length of channel ( $L^3 T^{-1} L^{-1}$ ). On the left hand side of Equation 2, the three terms represent unsteady flow, gradually varied flow, and the water surface slope, respectively. On the right hand side, the first two terms are defined above. The last term represents an acceleration resulting from the infiltration of water at the soil surface.

These two equations are commonly referred to as the Saint Venant equations. Mathematical models using the complete St. Venant equations have been formulated by Bassett and Fitzsimmons (1976), Katopodes and Strelkoff (1977), and Fonken et al. (1980). A discussion on the development of these mathematical models is given in Jensen (1980). According to Jensen, using the full St. Venant equations leads to "an accurate but computationally expensive and delicate model."

By neglecting the acceleration terms from the equation of motion, Equation 2 can be written as:

$$\frac{\partial y}{\partial x} = S_o - S_f \quad [3]$$

Equation 3 is the zero-inertia approximation (zero acceleration) to the equation of motion. The first mathematical model to simulate an irrigation event using zero inertia theory was developed by Katopodes and Strelkoff (1977). Later studies (Clemmens, 1979, Fangmeier and Strelkoff, 1979, and Elliot et al., 1982) have shown that the hydraulics of border and furrow irrigation can be accurately simulated by applying the zero-inertia assumptions.

If one assumes that the channel bottom slope is relatively steep, the surface depth gradient of Equation 3 becomes insignificant when compared to the other two terms. Upon deletion of the gradient term, Equation 3 reduces to:

$$S_o = S_f \quad [4]$$

Equation 4 is known as the normal depth approximation to the equation of motion. When the friction slope equals the field slope, uniform flow theory prevails and there exists a unique relationship between the depth and discharge. The properties of uniform flow are extensively examined in Chow (1959). Substitution of a depth-discharge relation into the continuity equation yields a kinematic-wave model. The mathematical derivation of kinematic-wave theory has been presented by Chen (1970) and also by Sherman and Singh (1982).

In order to develop simulation schemes more representative of field conditions, various researchers have expanded upon the last two models discussed above (zero inertia and kinematic-wave). Kibler and Woolhiser (1970) solved

the kinematic-wave equations for a variable slope profile. They developed this technique for flood routing purposes over a complex watershed. A series of planes at various elevations and slope gradients, termed a "cascade of planes", simulated the complex watershed. Kibler and Woolhiser (1970) used the outflow from a plane k-1 as the inflow hydrograph onto a plane k.

Wallender and Rayej (1984) incorporated variable values of Manning's roughness ( $n$ ) and variable shape factors (coefficients  $d$  and  $f$  in Equation 6) into a zero inertia model to simulate advance over wet and dry furrow sections. Using this technique, one can simulate changes that occur in the furrow's geometric properties after it has been wetted.

#### Kinematic-Wave Approximation

The first kinematic-wave model capable of simulating surge irrigation was presented by Walker and Lee (1981). The model was updated by Walker and Humphreys (1983) by utilizing a first-order Eulerian integration of the continuity equation. Walker and Humphreys chose the Manning equation as the unique stage-discharge relation. Manning's equation is:

$$Q = \frac{C}{n} A(R)^{.67} S_o^{.5} \quad [5]$$

In Equation 5,  $Q$ ,  $A$ , and  $S_o$  are as previously defined,  $R$  is the hydraulic radius ( $L$ ),  $n$  is Manning's roughness coefficient and  $C$  is a constant (1.0 in SI units and 1.49 in English units). For the remainder of this discussion, it is assumed that  $C$  equals 1.0 (working in SI units).

An empirical relation between the cross-sectional flow area and the channel properties of Equation 5 has been formulated by Elliot et al. (1982). This relation is:

$$d(A)^f = (AR^{.87})^2 \quad [6]$$

where  $d$  and  $f$  are empirical constants.

Substituting Equation 6 into 5 yields

$$Q = \frac{1}{n} A^{.5f} (dSo)^{.5} \quad [7]$$

By defining  $d$  as:

$$d = \frac{(dSo)^{.5}}{n} \quad [8]$$

and  $m$  as:

$$m = .5f \quad [9]$$

Equation 7 can be rewritten in the following form:

$$Q = dA^m \quad [10]$$

Equation 10 shows the flowrate to be a power relation of the flow area. Substitution of Equation 10 into the continuity equation (Equation 1) results in a partial differential equation having only two variables,  $A$  and  $Z$ . We have thus reduced the number of variables by one. Upon substitution, Equation 1 becomes:

$$\frac{\partial (dA^m)}{\partial x} + \frac{\partial A}{\partial t} + \frac{\partial Z}{\partial t} = 0 \quad [11]$$

#### Infiltration Models

In the modeling scheme of Walker and Humphreys (1983) and Izuno (1984), it is assumed that the infiltrated depth is a function of the infiltration opportunity time alone. In this way one can find the total derivative of the infiltrated depth with respect to time. Different researchers have used various empirical relationships for the function  $Z$ .

Walker and Lee (1981) employed the extended Kostikov relation to simulate infiltration over a dry section of furrow and a rate function for flow over a previously wetted section of furrow. The extended Kostikov equation is shown as Equation 12:

$$Z = kt^a + f_0 t \quad [12]$$

In Equation 12,  $Z$  is the infiltrated depth per unit area (L),  $t$  is infiltration opportunity time (T), and  $k$ ,  $a$ , and  $f_0$  are empirical coefficients fitted for the soil type. The first term on the right hand side of Equation 12 is a power function of time and is known as the time dependent intake rate. The term containing  $f_0$  is the constant or basic intake of the soil.

Hoping to achieve greater accuracy in simulating surge flow irrigation, Walker and Humphreys (1983) suggested the use of two extended Kostikov functions along with a transition function. An extended Kostikov equation was fitted for both a wet section of furrow and a dry section of furrow. Separate values of  $k$ ,  $a$ , and  $f_0$  were determined for both types of furrow sections. Walker and Humphreys assumed, based on field observations, that the infiltration rate did not drop instantaneously from the dry rate to the wet rate upon initial wetting. They introduced a transition function to modify the values of  $k$ ,  $a$ , and  $f_0$  to simulate this phenomenon. The transition function was based on the spatial distribution of advance for the surges of interest (namely surges  $n-2$ ,  $n-1$ , and  $n$ ). The reader is referred to the original work by Walker and Humphreys (1983) for a detailed account of their transition function. For the first surge over a dry furrow section, the dry intake rate equation was used. During the second surge over the same area, the values of  $k$ ,  $a$ , and  $f_0$  were modified by the transition function. Upon modification, the resulting values of  $k$ ,  $a$ , and  $f_0$  fell within the range of the dry intake rate

values and the wet intake rate values. During the third and subsequent surges, infiltration was characterized by the wet infiltration equation. Figure 1 shows the three types of furrow sections (dry, transition, and wet) and where they would occur for three subsequent surges, namely surges  $n-2$ ,  $n-1$ , and  $n$ .

Izuno (1984) employed the Clemmens branch function to model infiltration. The Clemmens branch function states that infiltration follows a time dependent rate curve until some time,  $t_b$ , at which time infiltration occurs at a constant rate. Equations 13 and 14 show the Clemmens branch function:

$$Z = kt^a, \quad t \leq t_b \quad [13]$$

and:

$$Z = kt_b^a + c(t - t_b), \quad t > t_b \quad [14]$$

where  $c$  is the basic intake rate (similar to  $f_o$ ) and  $t_b$  is the time at which the basic intake rate comes into effect.

Upon first inspection, Clemmens branch function appears to be discontinuous; however, continuity is assured because the value of the rate equation (first derivative) of Equation 13 will always equal  $c$  at the time  $t_b$ . Figure 2 displays the branch infiltration function proposed by Clemmens.

To model surge flow infiltration, Izuno (1984) proposed that after two surges had passed a given point, the infiltration rate would drop to the constant rate. This would occur regardless of whether or not  $t_b$  had been exceeded. Field observations supported his theory of this reduction in the infiltration rate when surging was practiced. For advance over a dry furrow section, Izuno (1984) employed the time dependent intake rate (Equation 13). During the passage of a second surge over a given point, Izuno (1984) , like

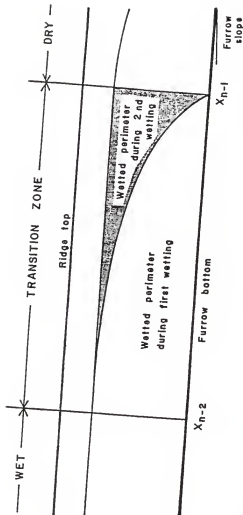


Figure 1. Furrow Longitudinal Section Showing Wetted Perimeter Differences Occurring Between Surges.  
Reproduced from Izumo (1984)

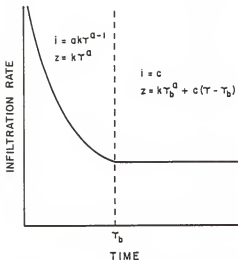


Figure 2. Clemmens Branch Infiltration Function  
Reproduced from Izuno (1984)

Walker and Humphreys (1983), used a transition function to modify the values of  $k$  and  $c$ . Unlike Walker and Humphreys (1983), however, Izuno (1984) did not modify the value of the exponent  $a$ . For advance over a wet section of furrow, the constant intake rate (Equation 14) simulated the soil's infiltration.

Unlike the spatially based transition function of Walker and Humphreys, Izuno based his transition relation on the opportunity time at the point of interest. The infiltration transition relationship of Izuno is written as:

$$Z = k't^a + c't \quad [15]$$

where:

$$k' = k - k(\text{OPP}_j) \quad \text{XTT}_{n-2} < \text{XA}_n \leq \text{XTT}_{n-1} \quad [16]$$

and:

$$c' = c(\text{OPP}_j) \quad \text{XTT}_{n-2} < \text{XA}_n \leq \text{XTT}_{n-1} \quad [17]$$

In Equations 15, 16, and 17,  $k'$  and  $c'$  are the modified Clemmens branch function coefficients.  $X_{TT_{n-2}}$  is the furthest advance of surge  $n-2$ .  $X_{TT_{n-1}}$  is the furthest advance of surge  $n-1$ , and  $X_{A_n}$  is the present advance of the current surge.  $OPP_j$  is the transition function which is a ratio of the opportunity time at a given point to the cycle time of the previous surge (surge  $n-1$ ).

$$OPP_j = \frac{OPT(n-1)_I}{T_{on}(n-1)} \quad [18]$$

where  $OPT$  is the infiltration opportunity time ( $T$ ) and  $T_{on}$  is the cycle time ( $T$ ) for the previous surge (surge  $n-1$ ). In Equations 16, 17, and 18, the  $I$  and  $J$  subscripts arise from the finite difference solution of the continuity equation (Equation 1). The  $J$  subscript refers to values which have been interpolated for the present computational nodal spacing while the subscript  $I$  denotes the computational nodal spacing of the previous surge. By basing the transition function solely on the infiltration opportunity time, the initial assumption that the infiltrated depth is a function of the opportunity time alone is satisfied. Izuno (1984) developed the  $OPP$  function to be linear in time but nonlinear with distance. Thereby, the nonlinearly decreasing opportunity times encountered as one approaches the leading edge of advance can be simulated.

### Numerical Solution Techniques

After selection of an appropriate time-based function to model the infiltrated depth,  $Z$ , the kinematic-wave equation can be solved. Equation 11 has been solved by two techniques, namely the method of characteristics and finite differences. The heart of the method of characteristics lies in the transformation of the partial differential equations into ordinary differential equations. An overview of the method of characteristics is given by Overton and

Meadows (1976).

The finite differencing schemes can be applied directly to the governing equations of motion. Solutions can be obtained by either an explicit or an implicit finite-difference form.

As presented by Walker and Humphreys (1983), the finite-difference integration of Equation 1 over time and space is:

$$\int_t^{t+\delta t} \left\{ \int_x^{x+\delta x} \frac{\partial Q}{\partial x} dx \right\} dt + \int_x^{x+\delta x} \left\{ \int_t^{t+\delta t} \frac{\partial A}{\partial t} dt \right\} dx \quad [19]$$

$$+ \int_x^{x+\delta x} \left\{ \int_t^{t+\delta t} \frac{\partial Z}{\partial t} dt \right\} dx = 0$$

which yields the first-order result:

$$\left\{ \tilde{Q}(x+\delta x, t) - \tilde{Q}(x, t) \right\} \delta t + \left\{ \bar{A}(x, t+\delta t) - \bar{A}(x, t) \right\} \delta x \quad [20]$$

$$+ \left\{ \tilde{Z}(x, t+\delta t) - \tilde{Z}(x, t) \right\} \delta x = 0$$

In Equation 20, the tilde superscript indicates that the values are spatially averaged over the distance  $\delta x$  and the bar superscript indicates time averaged values during the time  $\delta t$ .

Figure 3 shows a typical computational cell in the finite-difference scheme, showing integration over both the time  $\delta t$  (dashed lines) and the distance  $\delta x$ . In Figure 3, the subscripts J and M refer to the time step  $i-1$  while the subscripts L and R refer to the time step  $i$ . In a likewise fashion, L and J correspond to the distance  $x$  while M and R correspond to the distance

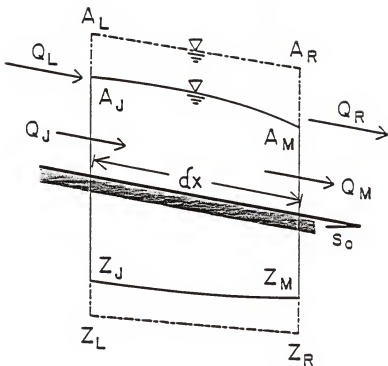


Figure 3. Computational Cell for Kinematic-Wave Model.  
Reproduced from Walker and Humphreys (1983)

$x \cdot \delta x$ . When Equation 20 is rewritten using the notation found in Figure 3, the resulting equation is:

$$\begin{aligned}
 & \left\{ \left\{ \theta Q_R + (1-\theta)Q_M \right\} - \left\{ \theta Q_L + (1-\theta)Q_J \right\} \right\} \delta t \\
 & + \left\{ \left\{ \phi A_L + (1-\phi)A_R \right\} - \left\{ \phi A_J + (1-\phi)A_M \right\} \right\} \delta x \\
 & + \left\{ \left\{ \phi Z_L + (1-\phi)Z_R \right\} - \left\{ \phi Z_J + (1-\phi)Z_M \right\} \right\} \delta x = 0
 \end{aligned} \tag{21}$$

where  $\theta$  is a time averaging coefficient and  $\phi$  is a space averaging coefficient (relating to the bar and the tilde, respectively, found in Equation 20). The values of  $\theta$  and  $\phi$  vary between 0.0 and 1.0 (Walker and Humphreys, 1983).

At nodes J, L, and M, the values of Q, A, and Z are known. At node R, Z is known since Z is only dependent upon time (t and  $\delta t$  are both known). Therefore, Equation 21 contains only two unknowns,  $Q_R$  and  $A_R$ . Using Equation 10 which relates flowrate to area, the number of unknowns can be reduced to one, either  $A_R$  or  $Q_R$ . According to Li et al. (1981), selecting Q as the independent variable will reduce the relative error in the calculation of A. Since the value of the exponent (m) in Equation 10 is greater than 1.0, if one solves for Q first and then computes A, the magnitude of any errors would be reduced. Conversely, if one solves for A first and then computes Q, any errors contained in the value of A will be magnified by the exponent m. According to the customs established in backwater computations, however, the flow area is generally chosen as the independent variable (Li et al., 1981). Writing Equation 21 in terms of  $A_R$  (after Walker and Humphreys, 1983), results

in:

$$A_R^m + C_1 A_R + C_2 = 0 \quad [22]$$

in which:

$$C_1 = \left\{ \frac{1-\theta}{\theta \Delta t} \right\} \frac{\delta x}{\delta t} \quad [23]$$

and:

$$\begin{aligned} C_2 = & -A_L^m + \left\{ \frac{1-\theta}{\theta} \right\} \left\{ A_M^m - A_J^m \right\} \\ & + \frac{\theta}{\theta \Delta t} \left\{ A_L + Z_L - A_J - Z_J \right\} \frac{\delta x}{\delta t} \\ & + \left\{ \frac{1-\theta}{\theta \Delta t} \right\} \left\{ Z_R - A_M - Z_M \right\} \frac{\delta x}{\delta t} \end{aligned} \quad [24]$$

Equation 22 is written for each cell and then solved by an iterative technique such as the Newton-Raphson scheme. For each successive time increment,  $\delta t$ , during advance, a new distance  $\delta x$  is calculated and added onto the time-distance grid. Figure 4 shows the solution process as it "marches" through time and space. As shown in Figure 4, each successive time step contains only one new advance distance. This holds true as long as the end of the field is not reached, the advance does not stall, or the inflow is not cutoff.

Prior to and during the initial time step, the values of  $A_J$ ,  $Z_J$ ,  $A_M$ ,  $Z_M$ ,  $A_R$ , and  $Z_R$  are zero. After completion of the initial time step, the flow has advanced a distance  $\delta x_1$ . At this time,  $A_L$  and  $Z_L$  will have been calculated. Hence, for this initial time step Equations 22-24 reduce to:

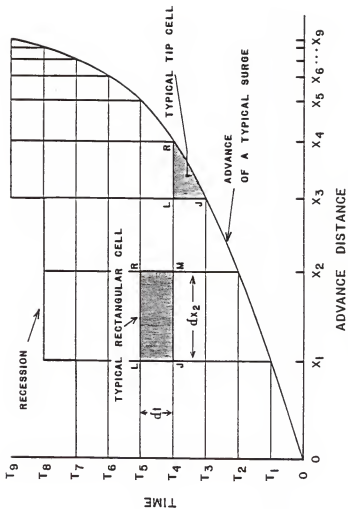


Figure 4. Time-Space Computational Grid.  
Reproduced from Walker and Humphreys (1983)

$$-A_L^m + \frac{\partial}{\partial t}(A_L + Z_L) \frac{\delta x_1}{\delta t} = 0 \quad [25]$$

Equation 25 can be solved to find the incremental advance distance  $\delta x$ . After the initial time step,  $Z_L$  can be calculated since it is assumed to be solely a function of time. The value of  $Q_L$  (and hence  $A_L$ ) is known from the inflow hydrograph into the field. Thus, the only unknown is the incremental advance distance. Solving for the advance distance yields:

$$\delta x_1 = \frac{\partial A_L^m \delta t}{\partial (A_L + Z_L)} \quad [26]$$

During each time increment  $\delta t$ , Equation 22 is solved for the new incremental advance  $\delta x$ .

Upon completion of advance, it is assumed that the flow leaves the field at the uniform flow depth. The last cell, for this case, is thus calculated as an interior cell (Walker and Humphreys, 1983).

After inflow is cut off, the kinematic-wave model presented by Walker and Humphreys (1983) is capable of simulating the recession of water across the field. Recession was defined as the time at which the flow area at any node falls below 5% of the inlet flow area (Walker and Humphreys, 1983). Either left and right end recession or left end recession and right end advance can be simulated by their model.

Several researchers have employed kinematic-wave theory to the modeling of surface irrigation and have attained admirable results. Figures 5 and 6 display the degree of accuracy achievable with the kinematic-wave modeling scheme. The input data used to generate Figures 5 and 6 can be found in Izuno (1984).

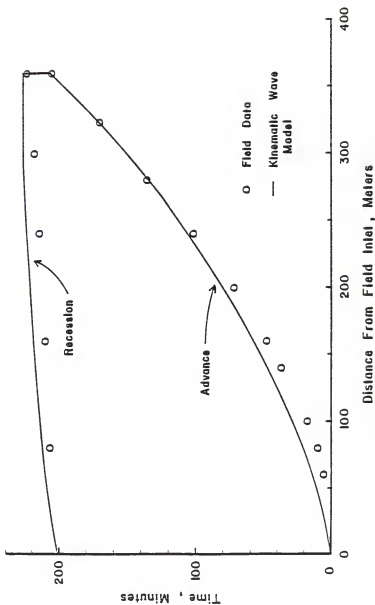


Figure 5. Kinematic-Wave Simulation of Continuous Flow Advance and Recession.  
(Kimberly Hard Farrow)  
Reproduced from Izuno (1984)

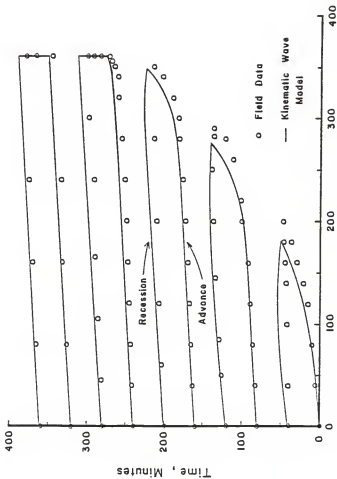


Figure 6. Kinematic-Wave Simulation of Surge Flow Advance and Recession.  
(Flowell Hard Furrow)  
Reproduced from Izumo (1984)

## INVESTIGATIONS

### Objectives

The objectives of the current study were threefold :

1. to expand the model of Walker and Humphreys (as modified by Izuno) to study the effects of a non-uniform slope profile and variable values of Manning's roughness ( $n$ ),
2. to incorporate the Soil Conservation Service's (SCS) design infiltration equation into the model of Walker and Humphreys, and
3. to optimize the surge irrigation strategy, by computer simulation, for selected soils in western Kansas.

### Field Studies

Field studies were conducted on three sites in southwestern Kansas. A pre-irrigation study was conducted on the Junior Leonard farm located approximately two miles south of Sublette, Kansas. Pre-irrigation and first irrigation studies were conducted on land managed by Frank Phief (owned by the Garden City Company) located approximately three miles north and four miles west of Holcomb, Kansas. First and second irrigation studies were conducted at the Garden City Experiment Station's Holcomb Experiment Field located approximately two miles north and three miles west of Holcomb, Kansas.

During mid-March, 1985, pre-irrigation studies were conducted on the Junior Leonard site. These studies were performed in cooperation with the Soil Conservation Service's (SCS) Target Area Team. The soil was a Richfield

silt loan with the rows under consideration being wheel trafficked.

A P&R Surge System's variable programmable valve was used to regulate direction of flow and cycle times. This valve uses an internal flapper to switch water between sets. When placed in its programmed mode, the P&R valve will calculate individual cycle times based on an estimated out-time. The out-time is defined as the required length of time for the majority of the water in the furrows to reach the field's end. The programmed cycle times are of variable duration, being calculated by the software in the valve. These cycle times were initially short, with each subsequent cycle time longer than the previous.

At Junior Leonard's site, the valve was used in its programmed mode. The out-time was set at 16 hours which resulted in on-times of 43, 57, 72, 86, 100, and 122 minutes. The inflow into the field was measured using one-inch throat width Parshall flumes.

To characterize the advance, flags were set at 15 minute increments. After the initial surge, the time required for the water to advance to the previously set flags was recorded. Upon reaching an unwetted section of furrow, flags were once again set at 15 minute increments.

Between surge on-times, the recession of water across the field was measured. The recession rate was found to be extremely difficult to characterize. The furrow had a rather large volume of dead surface storage remaining after inflow was cutoff. Since the recession rate was visually inspected, one had to estimate when recession was completed and the dead surface storage remained. On the fields under consideration, the surge off-times were usually long enough to allow this surface storage to infiltrate. Future studies did

not record the recession rate due to the difficulties associated with measuring it. Generally, the recession rate occurred quickly when compared to the advance rate.

Furrow cross-sectional profile measurements were taken with the aid of a scale and a drop rod. The scale was placed horizontally across the furrow and the vertical depths were read from the drop rod. The readings were taken at a two-inch horizontal spacing. These measurements were necessary to determine the relation between the furrow's hydraulic section and the cross sectional area. Replicates were made for a wetted (smooth) furrow section and a dry (rough) furrow section. These profiles were taken at a short distance from the head of the field.

Pre-irrigation studies at Frank Phief's location were conducted during early April, 1985. A P&R surge valve, similar to the one described above, was placed between the supply line and the gated pipe. During the pre-irrigation, a set of surge-flow tests and a set of continuous flow tests were conducted. The valve's program mode set the surge cycle on-times (estimated 36 hour out-time). The individual cycle times were calculated to be 97, 129, 162, 194, 227, and 272 minutes. Furrow profiles were taken using the same technique as on the Junior Leonard site.

During mid-July, first irrigation studies were conducted on this same field. Troubles with adjacent rows breaking over resulted in only one surge-flow test of variable cycle times. For this test, the out-time was set at 18 hours, which resulted in surge on-times of 43, 64, 81, 97, 113, and 137 minutes. One-inch throat width Parshall flumes were used to measure inflow into the field and runoff from the field's end. Field slope profile readings

revealed a major break in the slope at approximately 400 meters. Before the slope break, the field contained approximately a 0.17 percent slope. After the break, the slope increased to approximately 0.5 percent. At this site, all of the rows had some degree of wheel traffic on them.

First and second irrigation tests were conducted on the Garden City Experiment Station's Holcomb Experiment Field. During late July, first irrigation studies were performed. Second irrigation studies were conducted during the first week of September. Once again, a P&R Surge Systems valve was placed between the supply line and the gated pipe. The tests included continuous flow, uniform cycle times of 20, 60, and 120 minute on-times, and a variable cycle time. Two flowrates were studied, one being 1.64 liters per second and the other 1.07 liters per second. At this site, the orifice size was changed to control the inflow rate into the furrow. To ensure a constant inflow rate, Senninger pressure regulators were placed between the gated pipe openings and the orifice. These pressure regulators were activated at approximately 70 kilopascals.

Both compacted and noncompact furrows were studied. At the Holcomb site, more extensive runoff studies were conducted than at the previous two sites. Sixty degree V-notch flumes measured the runoff rates from the end of the field.

At this site, the differences between a dry, previously-unwetted furrow section and a previously-wetted furrow section were observed. These differences are shown visually in Figures 7 and 8. The dry furrow section was found to be much rougher than the wetted furrow section. The roughness differences were characterized and employed as Manning's "n" in the modeling scheme.



Figure 7. Dry, Rough Furrow Section,  
(Holcomb Experiment Field)



Figure 8. Previously Wetted, Smooth Furrow Section,  
(Holcomb Experiment Field)

These three field sites consisted of two different field lengths. The Leonard and Phief sites were approximately 800 meters long, while the Holcomb Experiment Field's length was approximately 300 meters long. Since little research has been conducted on the longer field lengths, the longer runs (800 meters) were desired.

Due to the large quantity of data that was collected during these tests, not all of it could be included. Data for selected sites and irrigation events can be found in Appendix A.

### Results of Field Studies

It was found that the advance rate across the field was relatively easy to characterize; however, the recession rate was not. After inflow cutoff, the furrows contained a relatively large volume of dead surface storage which required time to infiltrate. Due to this surface storage, the recession rate was difficult to follow. Generally, the time required for water to advance across the field was much longer than the time required for it to recede.

Upon following the advance rate, it was found that an accelerated advance rate existed for a previously wetted furrow section when compared to an unwetted section. This result, which was expected, occurred on all of the surge-flow plots. Figure 9 displays the accelerated advance rate for a selected furrow from Junior Leonard's site. This furrow received variable surge cycle on-times of 43, 57, 72, and 86 minute durations (out time = 16 hours). The inflow rate into the furrow was 2.65 liters per second. The initial surge required 33 minutes to advance the initial 200 meters while surges two, three, and four required between 12 to 15 minutes to rewet this same portion of the furrow. Upon reaching a dry section of furrow, the advance rate slows and follows a curve similar in shape to the initial surge advance rate curve. From Figure 9 it is apparent that during the second time a furrow section is wetted, the advance rate deviates slightly from the advance rate achieved after the furrow has been wetted for three or more surges. Similar trends were observed for all of the surge flow tests. This finding is in agreement with previous findings by other researchers. Both Walker and Humphreys (1983) and Izuno (1984) realized this phenomenon and modeled it by the addition of their transition function in the infiltration equation (refer to Figure 1).

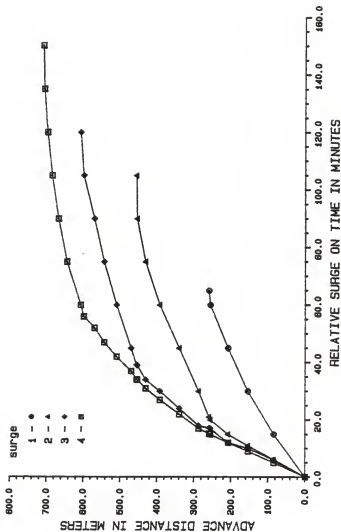


Figure 9. Advance Rate Acceleration Over a Previously Wetted Furrow Section Observed During Surge Flow, Non-Elasted Time Scale. (Junior Leonard Location, Pre-Irrigation, 1985)

During the pre-irrigation at Frank Phief's location, it was found that a large amount of variability existed between the advance rates for adjacent furrows when continuous flow was practiced. This variability is shown graphically in Figure 10. The total advance time for two adjacent rows to reach 725 meters ranged from 245 to 400 minutes. Part of this variability can be attributed to the different inflow rates; the south row receiving 3.41 liters per second and the north row receiving 3.09 liters per second. This 10 percent variation in the inflow rates, however, should not have been the only contributing factor for the 80 percent variation in advance distance. The advance rate variation found between these two furrows could be due to varying degrees of wheel compaction or a nonhomogeneous soil.

Figure 11 displays the surge-flow advance rate variations that were observed for two adjacent furrows on this field during the pre-irrigation. The cycle times were variable, being 97, 129, and 162 minutes. Inflow varied from 3.66 liters per second for the north row to 3.34 liters per second for the south row. The total on-time (not total elapsed time) for these furrows to advance to the field's end was 308 minutes and 322 minutes for the north row and the south row, respectively. Thus, a nine percent variation in the inflow rate resulted in only a five percent variation in the total on-time for advance completion. It is worthy to note that not all of the furrows (both surge flow and continuous flow) displayed these differences in the time required for advance completion.

For the continuous-flow furrows, the south row reached the field's end (field length = 792 meters) in 302 minutes while the north row had only reached 730 meters after 480 minutes. Comparing the surge-flow furrows to the continuous-flow south row, the surge flow resulted in a greater total on-time

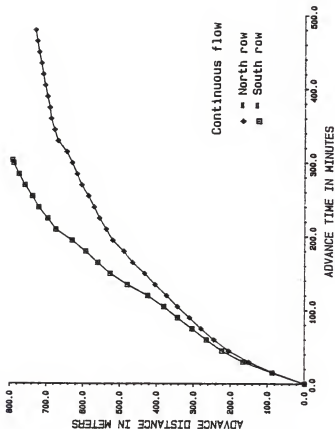


Figure 10. Advance Rate Variations Observed for Two Adjacent Compacted Furrows During Continuous Flow.  
(Frank Chief Location, Pre-Irrigation, 1985)

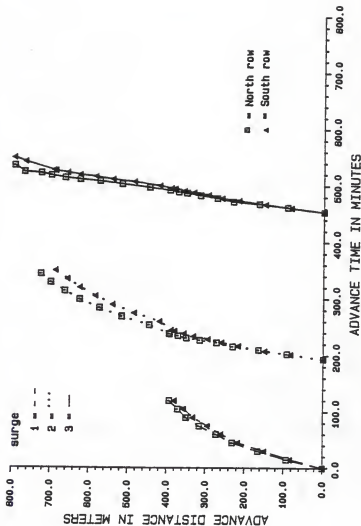


Figure 11. Advance Rate Variations Observed for Two Adjacent Compacted Furrows During Surge Flow.  
(Frank Chief Location, Pre-Irrigation, 1985)

to complete advance. However, it was observed that the continuous-flow's north row was more typical of the entire continuous-flow plot. The south row was somewhat of a fluke when compared to the other continuous-flow furrows of this field.

The effects of a break in the field slope on the resulting advance rate can be seen in Figure 10. At Frank Phief's location, a slope change existed at approximately 400 meters. At this point, the slope increased by a factor of three. The continuous-flow south row shows this break quite well with its speeded advance rate which occurs after 400 meters.

At the Holcomb Experiment Field, tests were conducted to study the effects of various surge on-times versus continuous flow. For the first and second irrigations of the season, the total water on-times for advance completion are shown in Tables 1 and 2, respectively. By multiplying these on-times by the inflow rate, 1.64 liters per second, the total volume of water required for advance completion can be found. The variable surge test consisted of six surges of 32, 43, 54, 64, 75, and 92 minutes. The mean value is the arithmetic average of four test rows.

For the first irrigation of the season, the variable surge on-times achieved advance completion in the least total on-time. For this treatment, advance was completed in 129 minutes (cumulative on-time).

During the second irrigation, the 120 minute surge on-times completed advance in the least total on-time, this being 120 minutes. It is interesting to note that the 120 minute surge on-times completed advance in 120 minutes. Thus, advance was completed during the first surge which would be similar to continuous flow. The effects of surging on the infiltration rate would not be

Table 1. Total On-Time for Advance Completion During the First Irrigation at the Holcomb Experiment Field.

Treatment	Mean Time -min
Continuous	180.
Surge 20	189.
Surge 120	152.
Surge Variable	129.

Table 2. Total On-Time for Advance Completion During the Second Irrigation at the Holcomb Experiment Field.

Treatment	Mean Time -min
Continuous	158.
Surge 20	170.
Surge 60	170.
Surge 120	120.
Surge Variable	157.

be present during the first surge. Thus, it is seen that during the second irrigation of the season at the Holcomb Experiment Field, surge flow did not produce any observed benefits.

### Simulation Studies

An existing kinematic-wave model was chosen to perform the simulations. This model was originally developed by Walker and Lee (1981), updated by Walker and Humphreys (1983), and modified by Izuno (1984). The final version of this model (Izuno's) was chosen to perform the simulations. This modeling scheme has been shown to accurately simulate furrow advance by both Walker and Humphreys (1983) and Izuno (1984). The model, as updated by Izuno, allows for the simulation of advance, recession and infiltration. Upon completion of the irrigation simulation, this model is capable of calculating various performance parameters and irrigation efficiencies. These include the Christiansen's uniformity coefficient, the application efficiency, the requirement efficiency, the tailwater percentage and the deep percolation percentage.

The model of Izuno was slightly modified so that it would fit and run on the Kansas State University Agricultural Engineering Department's DEC PDP 11 mini-computer. The model is written in FORTRAN 77 (f77) and compiled using the UNIX FORTRAN compiler (fc). The fc compiler is compatible with an f77 compiler, however, the fc compiler required fewer memory storage blocks for the compiled program code. The UNIX f77 compiler was found to produce too large of a compiled program code to run on the Agricultural Engineering's computer system.

As stated earlier, kinematic-wave theory can only be applied to sloping surfaces (furrows or borders) due to the normal depth approximation. Kinematic-wave theory assumes that the flowrate is uniquely related to the depth of flow, which in turn is related to the slope. If the slope is zero, the solution degenerates and the flowrate is zero (refer to Manning's equa-

tion, shown as Equation 5). Therefore, basin or flood irrigation on horizontal beds cannot be simulated using a kinematic-wave model.

The kinematic-wave model of Izuno (1984) was expanded to simulate the effects of a variable field-slope profile and variable values of the surface-roughness coefficient (Manning's  $n$ ). The need to model a variable surface-roughness arises from the geometric differences found between a dry versus a previously wetted furrow section. Wallender and Rayej (1984) implemented a similar type of function into a zero-inertia model and attained desirable results when compared to a model assuming a constant value of roughness. In the present version of the kinematic-wave model, two different roughness values are required as data. One value would characterize a dry furrow section and the other a previously wetted furrow section. The differences between the two types of furrow sections are shown in Figures 7 and 8. The numerical values of Manning's  $n$  were chosen by referencing Chow (1959) and through consultation with previous researchers.

For the initial surge or for continuous flow, the dry value of Manning's  $n$  is employed. After the initial surge, the function will check whether the current advance is over a dry or a wet furrow section. The appropriate value of Manning's  $n$  is then selected. The function that determines the value of Manning's  $n$  is also used to determine the current value of the slope. A method similar to Kibler and Woolhiser's (1970) "cascade of planes" is used. The outflow from a plane  $k-1$  is simulated as an inflow hydrograph onto a plane  $k$ . The effects of a kinematic shock formation were not examined in the current study.

At the exact point of the slope change, a discontinuity in the flow depth

will occur. This is due to the uniform flow approximation in the kinematic-wave model. Generally, the slope changes are of a small enough magnitude that this discontinuity should not adversely affect the resulting advance. It is advised that the time step in the finite differencing scheme be kept short (approximately one minute) so that the local errors arising from the slope change will be kept small.

In the current study, several methods were undertaken to find the values of  $a$ ,  $k$ , and  $c$  for the Clemmen's branch infiltration function. Books and design manuals were consulted for tabulated values of these coefficients; however, no such tables were found to exist.

A curve matching procedure, developed by Elliot et al. (1983a), was employed to find values of  $a$ ,  $k$ , and  $f_0$  for the extended Kostiaikov equation (Equation 12). The essence of Elliot's method follows. For a detailed account, please refer to the original work. Elliot employed zero-inertia theory to develop a model for an irrigation event. Holding the value of " $a$ " as a constant, the values of  $k$  and  $f_0$  were varied to generate dimensionless advance curves. The value of " $a$ " was then incremented a finite step and  $k$  and  $f_0$  were again varied to generate another set of curves. This technique was followed for discrete changes in  $a$  from 0.0 to 1.0 (the physical minimum and maximum limits for  $a$ ).

To determine  $a$ ,  $k$ , and  $f_0$  from this method, the advance distance and time must first be nondimensionalized and plotted on a scale similar to Elliot et al.'s (1983b). A curve-matching procedure of the advance versus time graph is then undertaken and the values of  $a$ ,  $k$ , and  $f_0$  are "backed out". For this procedure, continuous flow data is desired because of the large time scale,

which results in a greater number of points for matching purposes.

One shortcoming of this method is that any failures in the zero-inertia assumptions are carried over into the resulting values of  $a$  and  $k$ . A second shortcoming is that the value of  $f_o$  is found for an extended Kostinakov equation and not the Clemmens branch function.

The method employed to find the values of  $a$ ,  $k$ , and  $c$  are described by Izuno (1984). Using the inflow rate, the outflow rate, and the field length, a value of  $c$  can be determined. After a sufficiently long time from the start of an irrigation event, the outflow from the end of the field should reach a fairly constant value. Once this is reached, the value of  $c$  is found by:

$$c = \frac{\text{inflow} - \text{outflow}}{\text{field length}} \quad [27]$$

The values of  $a$  and  $k$  are then found by the curve matching procedure of Elliot et al. (1983b).

Because a constant outflow was not achieved in the tests, the value of  $c$  had to be modified slightly. Also, due to previously stated reasons, the "backed out" values of  $a$  and  $k$  were slightly modified to fit the advance data. Izuno (1984) states guidelines to be followed when adjusting these coefficients.

Because of the accelerated advance found with surge flow, it is theorized that the infiltration rate is lowered during surging. To model surge irrigation, Izuno (1984) theorized that the infiltration rate dropped to a constant rate after a furrow section has been wetted two times. Izuno's theory is shown graphically in Figure 12. When modeling surge infiltration, however, Izuno (1984) employed an opportunity-time-based transition function during the second wetting of a furrow section. An overview of this transition function

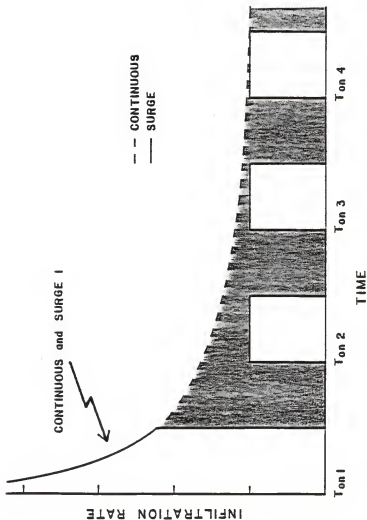


Figure 12. Reduction in Infiltrated Volume During Advance Under Surge Flow Resulting from a Step Drop to the Basic Infiltration Rate After the Initial Wetting.  
Reproduced from Izuno (1984)

can be found in the Literature Review section of this study. For a complete discussion, the reader is referred to the original work by Izuno (1984).

The Soil Conservation Service's design infiltration equation, as described in Jensen (1980), was incorporated into the model of Walker and Humphreys (1983). The SCS design equation for level borders and basins is:

$$Z = at^b + c \quad [28]$$

where  $c$  is a constant, equal to 7 millimeters. Values of  $a$  and  $b$  have been tabulated for various intake rate soils. These tables can be found in Jensen (1980). For furrow irrigation, the SCS procedure consists of multiplying the design equation by a factor to account for the furrow's shape. To find this factor, the value of the adjusted wetted perimeter must first be determined. The adjusted wetted perimeter accounts for the horizontal movement of water into the soil. According to Jensen (1980), the adjusted wetted perimeter is an empirical relationship and is found by:

$$P = 0.265 \left( \left( Qn/S_o^{0.5} \right)^{0.425} + 0.227 \right) \quad [29]$$

where  $P$  is the adjusted wetted perimeter (meters),  $Q$  is the flowrate (liters per second),  $n$  is Manning's roughness, and  $S_o$  is the furrow's slope (meter/meter). Equation 29 is then divided by the furrow spacing (in meters) to determine a ratio between 0.0 and 1.0. If the value of the adjusted wetted perimeter is numerically greater than the furrow spacing, it is set equal to the furrow spacing. In this way, the maximum value of the ratio is kept at 1.0.

Since the SCS design equation does not consider a constant infiltration rate, the effects of surge flow were modeled by considering the cumulative on- and off-times at a given point on the furrow section. The SCS infiltration rate was assumed to follow the time dependent curve at all times. Surge-flow

infiltration was modeled by determining an intake rate for an "extended" time period. This "extended" time period was equated to twice the opportunity time for a given furrow section. Using this "extended" time period, the new infiltration rate was calculated. Because the intake-rate curve is a decaying power relation, a lesser infiltrated volume was calculated by using the "extended" time value. Figure 13 displays the surge flow modeling strategy. As seen in Figure 13, the infiltration rate will continue to follow the time dependent curve. However, it follows this curve in discontinuous jumps.

An additional input variable was added into the model of Izuno (1984) to account for the two infiltration schemes. This variable is used to declare if infiltration will be simulated by Clemmens branch function or the SCS design equation. A program listing of the model can be found in Appendix B; Appendix B also contains sample input and output files.

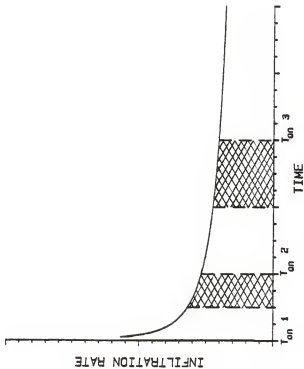


Figure 13. Reduction in Infiltrated Volume During Advance Under Surge Flow Resulting from the Effects of Cumulative On- and Off-Times.

## Results of Simulation Studies

The first irrigation at Frank Phief's location was simulated using the kinematic wave model of Izuno (1984) after it was modified to allow for a variable slope profile and variable values of Manning's  $n$ . The infiltrated depth was simulated by Clemmens branch infiltration function. The values of  $a$ ,  $k$ , and  $c$  were determined to be 0.28, 0.0171, and 0.0001, respectively, for time in minutes and infiltrated depth in meters. The wet roughness was set at 0.02 and the dry roughness at 0.03. The slope changes in distance from the head of the field and the corresponding slopes were:

Distance (meters)	Slope (percent)
0-244	0.185
244-365	0.155
365-640	0.536
640-792	0.451

The studies were conducted on two adjacent furrows during the first irrigation. Surge flow was used with variable on-times of 43, 57, 72, 86, and 100 minute durations. The north row received an inflow of 2.84 liters per second while the south row received 2.9 liters per second. The simulation results for the replicate surge flows are shown in Figures 14 and 15. As seen in Figure 14, the south row was accurately modeled. This result was expected since the values of  $a$ ,  $k$ , and  $c$  were fitted for this row. The predicted advance of the north row (Figure 15) has a relatively good fit; however, advance was overpredicted for surges four and five. For the fourth surge, the predicted advance distance was 646 meters; however, the actual advance distance for this surge was 579 meters. Thus, an 11 percent error is associated with this

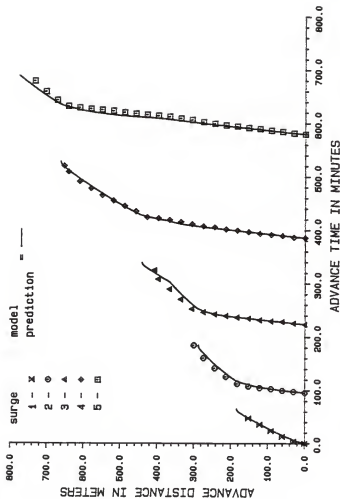


Figure 14. Kinematic-Wave Simulation of Surge Flow Advance Assuming a Variable-Slope Profile and Surface Roughness.  
(Frank Phief Location, South Row, First Irrigation, 1985)

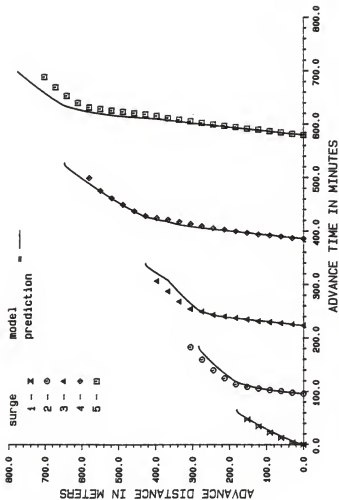


Figure 15. Kinematic-Wave Simulation of Surge Flow Advance Assuming a Variable-Slope Profile and Surface Roughness.  
(Frank Phief Location, North Row, First Irrigation, 1985)

surge. Surge five was found to contain a 10 percent error in advance; the predicted advance distance was 774 meters while the actual advance distance was 701 meters.

Part of these errors can be attributed to the different inflow rates of the north and south rows. The higher inflow rate of the south row results in a greater wetted perimeter when compared to the lower inflow rate of the north row. According to Izuno (1984), this greater wetted perimeter would effect the resulting values of  $a$ ,  $k$ , and  $c$  in the Clemmens branch function. Since the soil's intake rate is assumed to be solely time-dependent, the differences in the wetted perimeter would not be accounted for in the values of the intake coefficients. Because the Clemmens branch function was fitted for the advance of the south row, the resulting values of  $a$ ,  $k$ , and  $c$  may need modification to simulate the north row. When modeling the north row, the values of  $a$ ,  $k$ , and  $c$  were not modified because the inflow differences between the two rows were relatively small (0.06 liters per second).

The effects of the slope change on the model's predicted advance can be seen during surge three. The advance curves of Figures 14 and 15 are observed to increase beyond an advance distance of 365 meters, indicating that the advance rate accelerated after this point. As shown above, at this distance a major slope break occurred.

Figure 16 displays the model's fit by assuming the field had a constant value of slope and an average surface roughness (slope = 0.33 percent,  $n = 0.025$ ). Upon examination of Figure 16, it is seen that near the field slope break, the assumption of a constant slope leads to large errors in the predicted advance. For the second surge, the predicted advance distance was

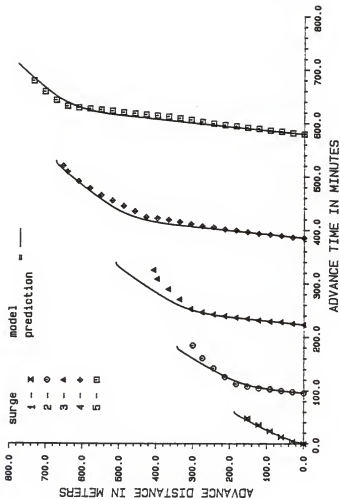


Figure 16. Kinematic-Wave Simulation of Surge Flow Advance Assuming a Constant-Slope Profile and Surface Roughness.  
(Frank Philef Location, South Row, First Irrigation, 1985)

343 meters, the actual advance distance being 300 meters. A 14 percent error is associated with this surge. The third surge's predicted advance was 509 meters, the actual advance was 406 meters. This represents a 25 percent error in the predicted advance. During the fourth surge, the constant slope model approaches reasonable accuracy, having an error of only three percent (actual advance of 652 meters, predicted advance of 671 meters). Near the slope break, it was found that the constant slope model tended towards relatively large errors in the predicted advance distance.

The north row was also simulated using the constant slope and surface-roughness model. Figure 17 displays the result of this simulation. Similar conclusions can be drawn for Figure 17 as were found for Figure 16. Once again, the advance distance is over predicted near the slope break.

Employing the variable slope and surface-roughness model used to calculate Figures 14 and 15, simulations were run to determine an optimum cycle time for surge flow. These simulations were made for the first irrigation at Frank Phief's location; therefore, they are somewhat site-specific. The cycle ratio was held at 0.5 and the inflow rate was set at 2.9 liters per second. Continuous flow was compared against surge flows of 30, 60, and 120 minute on-times. The results of these simulated runs are shown in Figures 18-21.

Upon examination of the simulated runs, it is seen that the predicted total time (on- and off-time) for advance completion was 608, 679, and 635 for the 30, 60, and 120 minute surge cycle on-times, respectively. Neglecting off-times, the cumulative on-times for advance completion were 286, 325, and 341 minutes for the 30, 60, and 120 minute surge cycle on-times, respectively. The variable cycle-time surge-flow test, conducted in the field, had a total

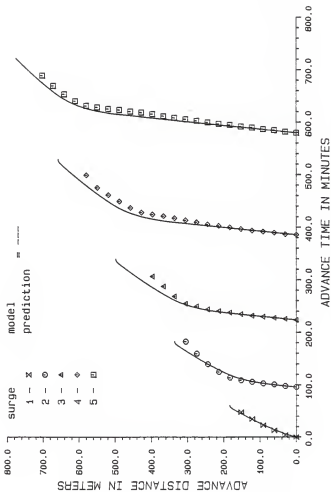


Figure 17. Kinematic-Wave Simulation of Surge Flow Advance Assuming a Constant-Slope Profile and Surface Roughness. (Frank Philef Location, North Row, First Irrigation, 1985)

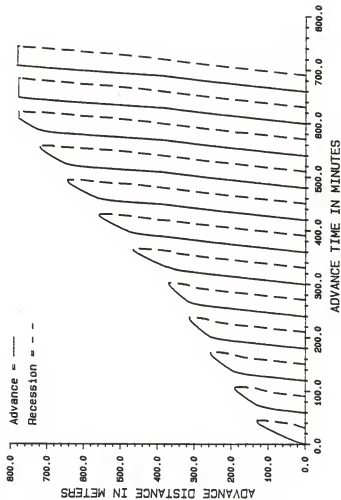


Figure 18. Model Simulation of Predicted Surge Flow Advance for 30-Minute Surge On-Times.  
(Frank Phief Location, South Row)

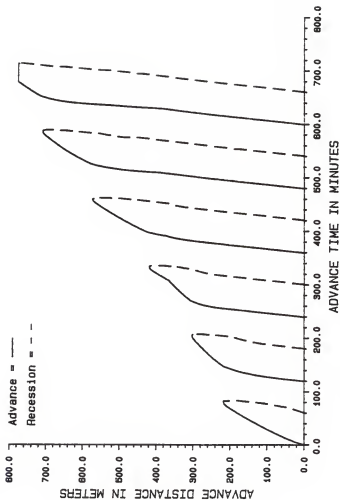


Figure 19. Model Simulation of Predicted Surge Flow Advance for 60-Minute Surge On-Times.  
(Frank Phief Location, South Row)

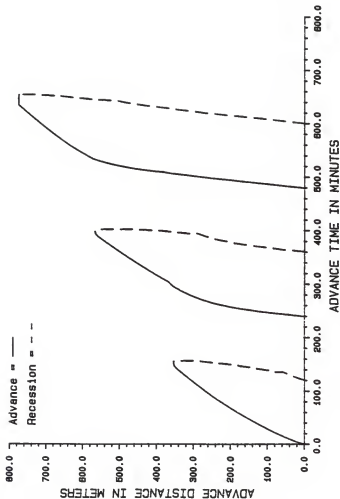


Figure 20. Model Simulation of Predicted Surge Flow Advance for 120-Minute Surge On-Times.  
(Frank Philef Location, South Row)

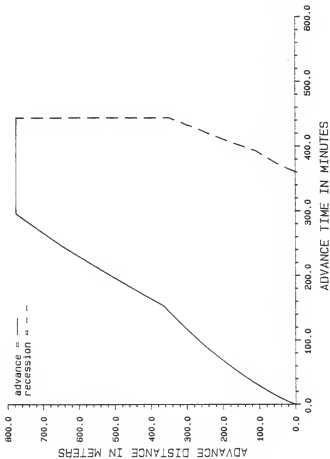


Figure 21. Model Simulation of Predicted Advance for Continuous Flow.  
(Frank Phief Location, South Row)

on-time of 342 minutes for advance completion. From the above tests, it is concluded that the 30-minute surge on-times resulted in the best surge irrigation strategy.

From the continuous-flow simulation, advance was completed in 296 minutes. This finding suggests that two of the three aforementioned surge-flow strategies resulted in a greater total on-time for advance completion. Based on his past experience, however, Frank Phief felt that surge flow completed advance in a shorter cumulative on-time than his usual method of continuous flow.

At the Holcomb Experiment Field, surge-flow simulations were conducted for the first irrigation of the season. In the Clemmens branch equation, the values of  $a$ ,  $k$ , and  $c$  were 0.33, 0.012, and 0.00013, respectively, for time in minutes and infiltrated depth in meters. The values of the intake coefficients were determined from the continuous-flow advance rate data. The inflow rate into the field was 1.64 liters per second. Three cycle times were studied; these consisted of 20 minute, 120 minute, and variable surge-flow on-times. From these simulations, the predicted advance completion occurred in cumulative on-times of 160, 221, and 229 minutes, respectively. Thus, the 20 minute surge-flow on-times yielded the quickest advance completion.

From the field studies at the Holcomb Experiment Field, the average cumulative on-times for advance completion were 189, 152, and 129 minutes for the 20, 120, and variable surge cycle on-times, respectively. Thus, in the field, the variable cycle on-times had completed advance in the least cumulative on-time. Upon comparison of the simulated studies with the field studies, a disagreement was found to exist in the best surge-flow cycle time. The simu-

lated studies favored the 20 minute on-time while the field studies suggest a variable on-time.

Simulation studies using the SCS design equation yielded questionable results. Upon consultation of the Finney county soil survey map (USDA-SCS, 1965), it was determined that the soil type at Frank Phief's location is a Richfield silt loam. The 1977 Kansas Irrigation Guide (USDA-SCS, 1977) states that the Richfield silt loam is in the 0.3-inch-per-hour intake family. Using the SCS infiltration equation, values of a and b were implemented for a 0.3-inch-per-hour intake rate (given in Jensen, 1980). Simulation studies were run for the first irrigation of the south row at Frank Phief's location. Results of this simulation are shown in Figure 22. As seen in Figure 22, the predicted advance is extremely poor. The predicted advance for surges one and two has an error greater than 100 percent. According to the simulation scheme using the SCS design equation, advance was completed in two surges. Because of the poor fit using the 0.3-inch-per-hour intake family, the values of a and b were increased to simulate a 0.5-inch-per-hour intake family. Again, an inaccurate simulation resulted. Advance completion was predicted after two surge on-times. The resulting advance versus time curve was similar to that found for the 0.3-inch-per-hour intake family (Figure 22).

Simulation studies for continuous flow at the Garden City Experiment Station's Holcomb Experiment Field were conducted using both the SCS design equation and Clemmens branch function. At the Holcomb Field, the soil type consists of Richfield and Ulysses silt loams (USDA-SCS, 1965). These soils had received deposits of silt and clay from previous year's irrigation water (Manges and Hooker, 1984). According to the Kansas Irrigation Guide (USDA-SCS, 1977), this soil lies within the 0.3- and the 0.5-inch-per-hour intake

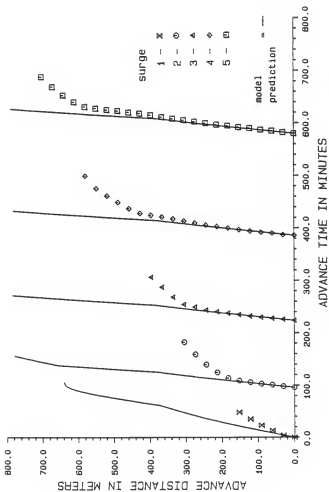


Figure 22. Model Simulation of Surge Flow Advance Using the SCS Design Equation With a 0.3 in/hr Intake Family.  
(Frank Phief Location, South Row, First Irrigation, 1985)

families.

Figure 23 displays the predicted advance for continuous flow using the Clemmens branch infiltration equation (second irrigation, hard furrow, inflow rate of 1.64 liters per second). As seen in Figure 23, a relatively good fit was achieved by this simulation. The values of  $a$ ,  $k$ , and  $c$  were 0.33, 0.012, and 0.00013, respectively, for time in minutes and infiltrated depth in meters.

Figure 24 shows this furrow's predicted advance using the SCS design equation with an intake family of 0.3-inches-per-hour. ( $a = 0.9246 \text{ mm/min}^b$ ;  $b = 0.720$ ). Once again, as seen in Figure 23, using the tabulated values of " $a$ " and  $b$  in the SCS design equation resulted in a poor fit of the advance. Increasing the values of " $a$ " and  $b$  to simulate a 0.5-inch-per-hour intake family resulted in little improvement of the predicted advance.

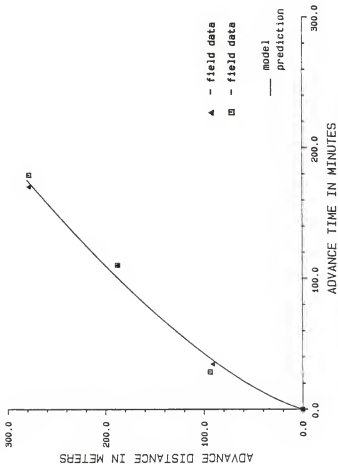


Figure 23. Model Simulation of Surge Flow Advance Using the Clemmens Branch Infiltration Equation.  
(Holcomb Experiment Field, Second Irrigation, 1985)

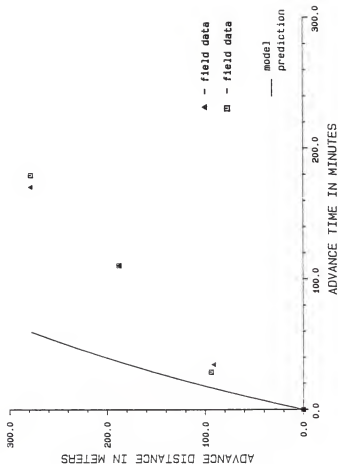


Figure 24. Model Simulation of Surge Flow Advance Using the SCS Design Equation With a 0.3 in/hr Intake Family.  
(Holcomb Experiment Field, Second Irrigation, 1985)

## DISCUSSION

Upon simulating the advance of irrigation water across the field, the model's performance was found to be sensitive to changes in the values of the intake coefficients. This fact was previously reported by Izuno (1984). A sensitivity analysis for the intake coefficients has been performed and is presented by Izuno (1984). For the above reason, the modeler must exercise caution when selecting the values of these coefficients. If erroneous values of the intake coefficients are used in the model, it can be guaranteed that the predicted advance distances will also be erroneous.

The addition of a variable slope and surface roughness subroutine into the kinematic-wave model (presented by Izuno, 1984) resulted in a more accurate simulation of the advance rate when major breaks in the field slope are present. This fact is shown in Figures 14-17. Using this subroutine, the maximum error found in the predicted advance distance was 11 percent. With the assumption of a constant slope and surface roughness, the advance distance's maximum error increased to 25 percent. For this assumption, the maximum error occurred near the field slope break.

Using the variable slope and variable surface-roughness subroutine, simulation studies were conducted for Frank Phief's field site and the Holcomb Experiment Field. Upon comparison of the simulated studies with the field studies, it was found that a disagreement exists in the best surge-flow cycle time. For the simulated tests at Frank Phiefs and the Holcomb Experiment Field, it was found that the shortest surge cycle on-times resulted in the optimum advance rate. Because these results were not observed in the field, the model was checked for possible errors or a failure in the kinematic wave

assumptions. It is believed that the surge-flow infiltration subroutine contains the problem.

Because it is assumed that the soil will reach its basic intake rate after two complete surge on-times, the shorter on-times result in sections of the furrow reaching the lower, constant-intake rate faster than would occur with the longer surge on-times. During the longer on-times, a greater amount of the advance will occur during the high, time-dependent intake rate and the relatively high transition intake rate. The increased volume of infiltrated water during these longer surge on-times results in less water being available to complete the advance.

A further shortcoming in the model's development is that the off-time effects are not fully accounted for in the infiltration subroutine. The infiltration subroutine as presented by Izuno (1984), is based solely on the cumulative on-time (opportunity time) for a given point. During inflow shut-off for the shorter surge cycle times, the surface stored volume of water in the furrow may not have sufficient time to completely infiltrate. If this occurs, the furrow sections with surface water still present during the next inflow on-time may not receive the reduced infiltration rate associated with surge flow. The model is incapable of predicting whether the dead surface storage will completely infiltrate during the off-time.

Besides modeling with Izuno's infiltration subroutine, simulations were conducted using the Soil Conservation Service's (SCS) design infiltration equation. It was found that the SCS's design infiltration equation does not accurately model surge infiltration when the intake coefficients are taken from the tabulated values. The SCS's method of grouping various soil types

under one intake family simplifies the design of irrigation systems; however, when simulating an irrigation event, more precise values of these coefficients are needed. This is partially due to the model's sensitivity to the values of the intake coefficients. As shown in Figures 22 and 24, using the intake coefficients found in the intake family tables led to an inaccurate prediction of advance. While the SCS intake family classification is an excellent means for characterizing a soil for design purposes, they appear to be too general to work for modeling purposes.

A possible shortcoming in the SCS design equation for modeling purposes is that it does not include a final constant-intake rate. Rather, the  $c$  term in the SCS equation represents an infiltrated depth due to surface storage. Previous researchers (Izuno, 1984, and Elliot et al., 1983) have found that the addition of a constant intake rate term leads to a more accurate simulation of advance. In the SCS design equation, if one neglects the addition of the  $c$  term ( $c$  is a constant set equal to seven millimeters), it is seen that this equation resembles the Kostikov infiltration equation, which is based solely on the time-dependent infiltration rate.

A second possible shortcoming associated with the SCS design equation is that the tabulated values of the intake coefficients were developed for design purposes. This being the case, they may contain an internal factor of safety to ensure that advance is completed. Any factor of safety designed into these coefficients is a potential cause of error in the simulated advance rate.

Potential errors may also exist in the accumulation of the off-times during the modeling of surge flow. In the present modeling scheme, after the initial surge the infiltrated volume is set equal to the volume that would

occur after twice the opportunity time at a given point. In other words, the effect of the off-time was set equal to the previous cumulative on-time. Since the SCS's infiltration equation was assumed to follow the time-dependent curve at all times, the addition of these off-times into the intake equation results in a lesser calculated-volume of infiltrated water. It may be that this off-time effect was assumed to be too large with the actual off-time effect being some fraction of the previous opportunity time for a given furrow section.

## CONCLUSIONS

In view of the objectives of this research, the conclusions are:

1. The addition of a non-uniform slope and variable surface-roughness subroutine into a kinematic-wave model increases the accuracy of the resulting advance distances. The increased accuracy is most pronounced when major breaks in the field slope are present.
2. The Soil Conservation Service's design infiltration equation has the potential to accurately model an irrigation event; however, the values of the intake coefficients should not be taken from the Intake Family tables. These tables have been generalized for a large family of similar soil types and do not appear to be site-specific enough for simulation purposes.
3. The surge irrigation strategy can be optimized by computer simulation; however, the resulting optimal strategy is valid only for the particular site modelled. Before an optimization can be performed for any soil type or seasonal condition, specific values of the intake-rate coefficients must be found.

## SUMMARY

Declining ground water tables in the Ogallala aquifer, combined with the rising costs of pumping water, are causing concern for the irrigators of western Kansas. Because of the declining water table and higher pumping costs, more efficient means of applying water are needed. For surface irrigation, surge flow presents itself as a potential water saver. In the current research, the effects of surge irrigation are studied through the use of a mathematical model of an irrigation event.

The objectives of the current study were to expand the kinematic wave model presented by Izuno (1984) to examine the effects of a variable slope profile and variable degrees of surface roughness, to incorporate the Soil Conservation Service's (SCS) design infiltration equation into the model, and to optimize, through computer simulation, the surge irrigation strategy for selected soils in western Kansas.

During the 1985 irrigation season, field studies were conducted at three locations in southwestern Kansas. These studies examined both surge and continuous irrigation flows. During these studies, the inflow rate, runoff rate, and advance rate were observed and recorded. The field data were first analyzed and then employed to calibrate a kinematic-wave model.

A variable slope and variable surface-roughness subroutine resulted in a more accurate prediction of advance when compared to an assumed constant slope and constant surface-roughness model. For the constant slope and surface-roughness model, a maximum relative error of 25 percent was observed in the predicted advance distance. In contrast, the variable slope and surface-roughness model resulted in a maximum relative error of 11 percent.

The kinematic-wave model was found to accurately model the test plot for which the intake coefficients were fit. Upon using these intake coefficients and varying the surge-flow on-times, it was found that the predicted advance rates did not agree with those observed in the field. Trends observed in the field data could not be reproduced by the model.

After trial simulations using the SCS's design infiltration equation with the intake coefficients taken from the Intake Family tables, it was found that the resulting simulation was poor. These coefficients appear to be too general for use in the kinematic-wave model. The SCS's method of grouping various soil types under a single intake family simplifies design work; however, this method appears to generalize the soil type too greatly for simulation purposes.

The kinematic-wave model was found to be sensitive to the values of the intake coefficients. Due to this sensitivity, it is difficult to optimize the surge irrigation strategy for a given soil type. Generally, the resulting optimization is specific for the soil type, soil location, and irrigation event (pre-irrigation, first irrigation, or second irrigation).

## SUGGESTIONS FOR FUTURE RESEARCH

Additional field work on the practice of surge irrigation is needed. Although current research has shown surge flow to be effective, it has also shown that surge flow can have a detrimental effect on certain types of soil conditions. Studies involving various soil types, soil compactions, irrigation number, and surge strategy would shed insight as to where and when surge flow should be practiced. In addition to studying the advance rate, runoff rate, inflow rate, and furrow shape; extensive studies are needed on the distribution and volume of infiltrated water.

This additional field work could provide a more accurate calibration of the kinematic-wave model. This work would also aid in refining the existing intake subroutines or in developing a new intake subroutine. Because the intake subroutines studied were solely time dependent; a new intake subroutine might want to examine the effects of wetted perimeter differences, surface sealing, air entrapment, soil hysteresis, or a two dimensional infiltration flux (for furrow irrigation).

## REFERENCES

- Bassett, D. L. and D. W. Fitzsimmons. 1976. Simulating overland flow in border irrigation. Transactions of the ASAE 19(4): 674-680.
- Bassett, D. L., B. E. Bowe, G. J. Weatherly, and R. G. Evans. 1983. Furrow performance under temporally varied inflow. ASAE Paper No. 83-2015
- Bishop, A. A., W. R. Walker, N. L. Allen, and G. J. Poole. 1981. Furrow advance rates under surge flow systems. Journal of the Irrigation and Drainage Division, ASCE 107(IR3): 309-324
- Chen, C. 1970. Surface irrigation using kinematic-wave method. Journal of the Irrigation and Drainage Division, ASCE 96(IR1): 39-46
- Chow, V. T. 1959 Open channel hydraulics. McGraw-Hill Book Company. New York, New York.
- Clemmens, A. J. 1981. Evaluation of infiltration measurements for border irrigation. Agricultural Water Management 3(4): 251-267
- Clemmens, A. J. 1979. Verification of the zero-inertia model for border irrigation. Transactions of the ASAE 22(6): 1306-1309
- Coolidge, P. S., W. R. Walker, and A. A. Bishop. 1982. Advance and runoff-surge flow furrow irrigation. Journal of the Irrigation and Drainage Division, ASCE 108 (IR1):35-42.
- Elliot, R. L., W. R. Walker, and G. V. Skogerboe. 1982. Zero-inertia modeling of furrow irrigation advance. Journal of the Irrigation and Drainage Division, ASCE 108(IR3): 179-195.
- Elliot, R. L., W. R. Walker, and G. V. Skogerboe. 1983a. Infiltration parameters from furrow irrigation advance data. Transactions of the ASAE:1726-1731.
- Elliot, R. L., W. R. Walker, and G. V. Skogerboe. 1983b. Furrow irrigation advance rates : A dimensionless approach. Transactions of the ASAE:1722-1725.
- Fangmeier, D. D. and T. Strelkoff. 1972. Mathematical models and border irrigation design. Transactions of the ASAE 22(1): 93-99.
- Fonken, D. W., T. Carmody, E. M. Laursen, and D. D. Fangmeier. 1980. Mathematical model of border irrigation. Journal of the Irrigation and Drainage Division, ASCE 106(IR3): 203-219.
- Izuno, F. T. 1984. Surge irrigation : characterization of advance, infiltration and performance for irrigation management. Unpublished Ph.D. Dissertation, Department of Agriculture and Chemical Engineering, Colorado State University, Fort Collins. Colorado

- Izuno, F. T. and T. H. Podmore. 1984. Surge irrigation management. ASAE Paper No. 84-2592
- Jensen, M. E. (Ed.). 1980. Design and operation of farm irrigation systems. Monograph, American Society of Agricultural Engineers, St. Joseph, Michigan.
- Katopodes, N. D. and T. Strelkoff. 1977. Hydrodynamics of border irrigation-complete model. Journal of the Irrigation and Drainage Division, ASCE 103(IR3): 309-324.
- Kibler, D. F. and D. A. Woolhiser. 1970. The kinematic cascade as a hydrologic model. Hydrology Papers. Colorado State University, Fort Collins, Colorado. (39) 27p.
- Li, R., D. B. Simmons, and M. A. Stevens. 1975. Nonlinear kinematic wave approximation for water routing. Water Resources Research. American Geophysical Union. 11(2): 245-252
- Manges, H. L. and M. L. Hooker. 1984. Field comparison of continuous, surge and cutback irrigation. ASAE Paper No. 84-2093
- Overton, D. E. and M. E. Meadows. 1976. Stormwater modeling. Academic Press, New York, New York.
- Podmore, T. H., Duke, H. R. and F. T. Izuno. 1983. Implementation of surge irrigation. ASAE Paper No. 83-2018.
- Sherman, B. and V. P. Singh. 1982. A kinematic model for surface irrigation: an extension. Water Resources Research 18(3): 659-667.
- Stringham, G. E. and J. Keller. 1979. Surge flow for automatic irrigations. Irrigation and Drainage Specialty Conference. ASCE. July 10p.
- USDA-SCS. 1965. Soil survey--Finney County, Kansas. Series 1961, No. 30. U. S. Government Printing Office, Washington, DC.
- USDA-SCS. 1977. Irrigation guide--Kansas. IG Notice KS-6, 10-19-79
- Walker, W. R. and A. S. Humpherys. 1983. Kinematic wave furrow irrigation model. Journal of the Irrigation and Drainage Division, ASCE 109(4): 377-392
- Walker, W. R. and T. S. Lee. 1981. Kinematic-wave approximation of surged furrow advance. ASAE Paper No. 81-2544
- Wallender, W. W. and M. Rayej. 1984. Zero-inertia surge model with wet-dry advance. ASAE Paper No. 84-2593.

## APPENDIX A

## SELECTED FIELD DATA

Table 3. Furrow Inflow Rates.

Site	Inflow lps
Leonard	2.65
Phief	
Pre-Irrigation, Continuous	
North Row	3.09
South Row	3.41
Pre-Irrigation, Surge	
North Row	3.34
South Row	3.66
First Irrigation, Surge	
North Row	2.84
South Row	2.90

Table 4. Surge Flow On-Times for Variable Cycle Times.

Site	On-Time min
Holcomb	
Surge	
1	32
2	43
3	54
4	64
5	75
6	92
Leonard	
Surge	
1	43
2	57
3	72
4	86
Phief	
Pre-Irrigation	
Surge	
1	97
2	129
3	162
First Irrigation	
Surge	
1	43
2	57
3	72
4	86
5	100
6	122

Table 3. Pre-Irrigation Advance Times for Variable Surge  
On-Times at the Junior Leonard Site.

Distance m	On-Time -min Surge			
	1	2	3	4
0.	0.	0.	0.	0.
85.	15.	6.	6.	5.
155.	30.	11.	10.	9.
208.	45.	15.	12.	12.
256.	60.	20.	17.	15.
259.	65.	21.	17.	15.
287.		30.	18.	17.
340.		45.	24.	22.
392.		60.	30.	27.
431.		75.	34.	31.
454.		90.	39.	34.
455.		105.	39.	34.
470.			45.	37.
509.			60.	42.
543.			75.	47.
569.			90.	52.
598.			105.	56.
606.			120.	60.
643.				75.
666.				90.
684.				105.
696.				120.
705.				135.
707.				150.

Table 6. Advance Distances for Continuous Flow  
at the Holcomb Experiment Field.

Time min	Distance m
First Irrigation	
0.	0.
29.	94.
111.	188.
180.	278.
Second Irrigation	
0.	0.
35.	91.
111.	187.
171.	278.

Table 7. Total Cumulative On-Times for Advance Completion at the Holcomb Experiment Field.

Treatment	Total Time -min Replicate			
	1	2	3	4
First Irrigation				
Continuous	180.	171.	152.	152.
Surge 20	120.	120.	120.	120.
Surge 120	129.	171.		
Surge Variable	189.	212.		
Second Irrigation				
Continuous	219.	154.	119.	135.
Surge 20	160.	160.	180.	180.
Surge 60	180.	160.	180.	160.
Surge 120	120.	120.	120.	120.
Surge Variable	179.	129.	193.	129.

Table 8. Pre-Irrigation Advance Distances for Continuous Flow at the Frank Chief Site.

Time min	Distance -m	
	South Row	North Row
0	0.0	0.0
15	87.1	85.3
30	166.4	149.7
45	223.7	204.8
60	265.5	244.5
75	304.2	279.8
90	343.5	310.9
105	380.7	343.5
120	424.6	373.1
135	480.1	404.5
150	526.7	432.8
165	560.5	465.4
180	593.4	488.9
195	630.3	519.7
210	674.5	537.4
225	696.5	555.7
240	721.5	570.0
255	738.2	585.8
270	758.6	604.1
285	775.1	616.6
300	789.4	629.7
304	792.5	
315		644.7
330		668.4
345		677.9
360		687.0
375		691.0
390		697.0
405		703.5
420		709.0
435		714.1
450		720.2
465		725.4
480		730.0

Table 9. Pre-Irrigation Advance Times Observed for the North Row at the Frank Phief Site.

Distance m	Time -min Surge		
	1	2	3
0.	0.	0.	0.
93.	15.	9.	8.
166.	30.	16.	14.
231.	45.	22.	18.
273.	60.	29.	24.
316.	75.	33.	29.
350.	90.	37.	33.
372.	105.	41.	35.
394.	120.	44.	38.
395.		45.	38.
446.		60.	43.
516.		75.	49.
573.		90.	54.
624.		105.	57.
662.		120.	60.
699.		135.	64.
725.		150.	68.
768.			70.
793.			81.

Table 10. Pre-Irrigation Advance Times Observed for the South Row at the Frank Chief Site.

Distance m	Time -min Surge		
	1	2	3
0.	0.	0.	0.
82.	15.	8.	7.
148.	30.	14.	13.
216.	45.	23.	20.
259.	60.	29.	24.
294.	75.	35.	30.
331.	90.	40.	34.
355.	105.	45.	37.
379.	120.	49.	41.
389.		51.	42.
419.		66.	46.
483.		81.	53.
539.		96.	57.
583.		111.	62.
623.		126.	65.
655.		141.	69.
685.		156.	72.
691.			73.
764.			88.
793.			95.

Table 11. First Irrigation Advance Times Observed for the North Row at the Frank Phief Site.

Distance ■	Time -min Surge				
	1	2	3	4	5
0.	0.	0.	0.	0.	0.
31.	4.	2.	2.	1.	2.
61.	13.	5.	4.	4.	5.
91.	23.	7.	6.	6.	7.
121.	35.	10.	8.	8.	10.
152.	48.	13.	11.	11.	12.
183.		18.	14.	14.	15.
213.		29.	17.	17.	17.
244.		44.	20.	20.	20.
274.		64.	26.	24.	23.
305.		87.	31.	28.	26.
335.			45.	32.	29.
366.			64.	36.	32.
396.			83.	39.	36.
427.				43.	39.
457.				52.	41.
488.				64.	44.
518.				76.	46.
549.				90.	49.
579.				114.	52.
610.					61.
640.					74.
671.					90.
701.					109.

Table 12. First Irrigation Advance Times Observed for the South Row at the Frank Phief Site.

Distance #	Time -min Surge				
	1	2	3	4	5
0.	0.	0.	0.	0.	0.
31.	4.	2.	2.	1.	2.
61.	13.	4.	5.	4.	5.
91.	24.	7.	6.	6.	7.
122.	36.	9.	8.	8.	10.
152.	48.	12.	11.	11.	12.
183.		17.	13.	14.	15.
213.		30.	16.	16.	17.
244.		46.	19.	20.	20.
274.		65.	23.	22.	23.
300.		89.			
305.			29.	26.	27.
335.			47.	30.	30.
366.			66.	34.	33.
396.			85.	37.	35.
406.			102.		
427.				39.	37.
457.				50.	39.
488.				60.	41.
518.				70.	44.
549.				90.	46.
579.				93.	48.
610.				106.	50.
640.				124.	53.
652.				135.	
671.					64.
701.					80.
732.					100.

Table 13. Field Elevations at the  
Frank Phief Site.

Distance m	Elevation m
0.	31.36
31.	31.27
61.	31.19
91.	31.14
122.	31.09
152.	31.06
183.	31.01
213.	30.92
244.	30.90
274.	30.90
305.	30.84
335.	30.77
366.	30.73
396.	30.66
427.	30.54
457.	30.34
488.	30.17
518.	30.03
549.	29.84
579.	29.62
610.	29.45
640.	29.31
671.	29.15
701.	29.00
732.	28.90
762.	28.80
777.	28.78

## APPENDIX B

COMPUTER VARIABLE DEFINITIONS, PROGRAM LISTING, AND  
SAMPLE INPUT AND OUTPUT FILES

## COMPUTER VARIABLE DEFINITIONS

A	Exponent in the time dependent portion of the infiltration function
ALPHA	Coefficient in the unique stage-discharge relationship
AMM1	AMP1 - 1
AMP1	Exponent in the unique stage-discharge relationship
AN	Array of cross-sectional flow area at the end of the new time step in the finite difference scheme, $m^2$
AP	Array of cross-sectional flow area at the end of the previous time step in the finite difference scheme, $m^2$
AO	Cross-sectional flow area at normal depth corresponding to the inflow rate, $m^2$
CONK	Coefficient in the time dependent portion of the infiltration function, $m^3/m^2/min^a$ or $m^3/m/min^a$
CYTIME	Array of inflow cycle on-times for each surge, min
C1	Coefficient in the simplification of the first-order Eulerian integration of the continuity equation
C2	Coefficient in the simplification of the first-order Eulerian integration of the continuity equation
D	Coefficient in the hydraulic section-area relationship
DAK	Incremental adjustment factor for flow area computations in the Newton-Raphson solution technique
DAN	Previous value of flow area, used in the Newton-Raphson solution technique
DIST	Array representing the distances from the field inlet of each 5 m station downfield, m
DT	Time increment used in the finite difference scheme, sec
DTM	Time increment used in the finite difference scheme, min
DISTN	Number of points in UCC calculations

DP	Deep percolation occurring at each 5 m station downfield, $m^3/m$
DPP	Deep percolation percentage expressed as a decimal
DTZT	Array of total infiltration for an irrigation occurring at 5 m stations downfield, $m^3/m$
DXA	Linear interpolation ratio used to convert nodal values of infiltration to 5 m spacings
DX	Array of incremental advance distances occurring between time steps, m
EA	Irrigation application efficiency, percent
ER	Irrigation requirement efficiency, percent
F	Exponent in the hydraulic section-area relationship
FL	Field length, m
FO	Basic intake rate in the branch infiltration function, neglected in the SCS infiltration subroutine, $m^3/m^2/min$ or $m^3/m/min$
FSPACE	Furrow spacing, m
IFL	Integer value of field length, m
IJK	Counter of number of surges completed
INFIL	Infiltration back-out or evaluation suppression option indicator (1 - suppress evaluation, 2 - complete)
INPMOD	Indicator specifying whether more than one simulation will be run from a single data file (1 - next data set, 0 - stop)
IPAO	Post advance option selection variable (1 - surge, 2 - continuous)
K	Loop counter, also used as a flag variable for initial advance infiltration
MAX	Maximum number of cells in the finite-difference solution technique
NCELL	Counter of the number of computational cells in the finite difference scheme
NSURG	Total number of surges to be run

NSOCHG	Total number of slope changes
OPP	Value of the opportunity time ratio OPTRAT interpolated to node spacings of present surge
OPT	Array of opportunity times at each node for the previous surge for use in the surge infiltration transition function
OPTRAT	Array of opportunity times at each node for the previous surge divided by the total on-time for that surge for use in the surge infiltration transition function
PHI	Space averaging constant set to equal 0.65
QIN	Array of inflow rates for each surge, $m^3/m/sec$ or $m^3/m^2/sec$
QJ	Inflow at the left boundary of the finite difference computational cell at the $i$ th time step, $m^3/m/sec$
QL	Inflow at the left boundary of the finite difference computational cell at the $i-1$ time step, $m^3/m/sec$
QM	Outflow at the right boundary of the finite difference computational cell at the $i-1$ time step, $m^3/m/sec$
REQ	Irrigation requirement, $m^3/m^2$
ROFF	Accumulator of the volume of runoff occurring during an irrigation, $m^3/m$
RUFN(1)	Manning's roughness coefficient for the rough furrow section, $n$
RUFN(2)	Manning's roughness coefficient for the smooth furrow section, $n$
SCHEME	Specifies the infiltration subroutine, either 'csu' or 'scs'
SO	Array of field slopes, $m/m$
TA	Array of advance times, $sec$
TB	Time when basic intake rate comes into effect after the natural decay of the time dependent intake function, $min$
TBASIC	TB rounded to the nearest whole number

TCO	Inflow cutoff time for each surge, sec
TCOM	Time of system cutoff, min
TDX	Array of incremental advance distance between nodes, m
TEMP1	Temporary dummy variable set equal to CONK
TEMP2	Temporary dummy variable set equal to F0
THETA	Time-averaging constant set equal to 0.65
TMAX	Maximum time allowed for advance phase completion, sec
TMAXM	Maximum time allowed for advance phase completion, min
TO	Array of times that water covers each furrow section corresponding to the computational nodes, sec
TR	Array of recession times for each computation node, sec
TWP	Tailwater percentage expressed as a decimal
TZT	Array accumulating prior infiltration at each node with new infiltration from the present surge, $m^3/m$
T1	Array of advance times at nodes, min
T2	Array of recession times at nodes, min
UCC	Christiansen's uniformity coefficient
VDP	Total volume of deep percolation per furrow, $m^3/m$
VINF	Total volume of infiltration per furrow, $m^3/m$
VOLAP	Total volume of water application per furrow, $m^3/m$
VREQ	Total volume of irrigation requirement per furrow, $m^3/m$
VTW	Total volume of runoff per furrow, $m^3/m$
VWSTO	Total volume of water stored per furrow, $m^3/m$
WSTO	Volume of water stored in the root zone at each 5 m station, $m^3/m$
W1	Array containing the description of a particular simulation exercise
XA	Array of advance distances, m
XAPRE	Array of nodal values of advance distances for the

	previous surge for use in the surge infiltration transition function, m
XSOCHG	Distance from head of field to field slope changes, m
XT	Array of advance distances for each node during the Previous surge, m
XTT	Array of the total advance distances for each surge, m
YAVE	Average DTZT in UCC calculations
YTOT	Temporary summation of DTZT in UCC calculations
YY	Temporary summation of (DTZT-YAVE) in UCC calculations
ZN	Infiltration cross-sectional area for the end of the new time step in the finite difference scheme, m <sup>2</sup>
ZP	Infiltration cross-sectional area at the end of the previous time step in the finite difference scheme, m <sup>2</sup>

## PROGRAM LISTING

COLORADO STATE UNIVERSITY  
VERSION 5, APRIL, 1983

(REVISED 1986)  
(KANSAS STATE UNIVERSITY)

UNIFORM FLOW SURFACE IRRIGATION (SURGE FLOW) MODEL  
WITH EVALUATION CAPABILITY

\*\*\*\*\*  
\*\*\*\*\*  
INPUT DATA AND CONTROLS  
\*\*\*\*\*

INPMOD = Input Control, 0=Stop and 1=New Metric Data  
W1 = Name of Problem in Less Than 66 Characters  
RUFN(1) = Dry Manning's Roughness, n  
RUFN(2) = Wet Manning's Roughness, n  
FL = Field Length in m  
DTM = Delta Time in Minutes  
D, F = Furrow Geometry Parameters D and F  
Where  $A^{**2} * R^{**4/3} = D * A^{**F}$   
FSPACE = Furrow Spacing in M  
TCOM = Time of System Cut-Off in Minutes  
TMAXM = Maximum Time of Advance in Minutes  
QIN = Inflow in  $M^{**3}/SEC/M$   
CYTIME = Surge Cycle On-Time in Minutes  
NSOCHG = Maximum Number of Slope Changes  
XSOCHG = Distance From Head of Field to Slope Change in M  
SO = Slope of Field in M/M  
SCHEME = Infiltration Modeling Scheme, Either 'CSU' Or 'SCS'  
A = Infiltration Exponent A  
CONK = Infiltration Multiplier in Time-Dependent Equation  
in  $M^{**3}/M^{**2}/MIN$  or  $M^{**3}/M/MIN$   
FO = Branch Function Basic Intake Rate in  $M^{**3}/M^{**2}/Min$   
IPAO = Post Advance Option, 1 = Surge, 2 = Continuous  
INFIL = Infil Backout Option, 1 = Suppress Evaluation,  
2 = Complete Evaluation  
REQ = Irrigation Requirement in  $M^{**3}/M$

```

C
C
parameter (max=300)
common/a/ ncell, xt(0:max), kb, tdx(0:max)
common/b/ xa(0:max), tzt(0:max)
common/c/ dist(0:max), dt
common/d/ iflfiv, dtzt(0:max), nsochg, d
common/e/ nsurg, cytime(20), qin(20), req, roff, fl
common/f/ to(0:max), ta(0:max), tr(0:max), opt(0:max)
common/g/ xapre(0:max), xtt(0:20), xsochg(30), so(30)
common/h/ rufn(2), fspace, iii, t, ijk, zn(0:max), j, ipao
common/i/ conk, fo, a, optrat(0:max), tbasic, temp1, temp2
dimension ap(0:max), an(0:max), zp(0:max), t2(0:max),
$      dx(0:max), t1(0:max)
character*4 w1(16)
character*3 scheme

C
C      *****
C      Read Values of Input Data
C      *****
C
1 read( 5,* ) inpmod
  if (inpmod .eq. 0) stop
  read( 5,8011 ) w1
  read( 5,* ) rufn(1), rufn(2), fl
  read( 5,* ) dtm
  read( 5,* ) d, f
  read( 5,* ) fspace
  read( 5,* ) tcom, tmaxm
  read( 5,* ) nsurg
  do 20 i = 1, nsurg
20 read( 5,* ) qin( i ), cytime( i )
    read( 5,* ) nsochg
    do 30 i = 1, nsochg
30 read( 5,* ) xsochg(i), so(i)
    read( 5,8008 ) scheme
    read( 5,* ) fo, conk, a
    read( 5,* ) ipao, infil
    read( 5,* ) req

C
C      *****
C      Print Values of Input Data
C      *****
C
write( 6,8013 )
write( 6,8012 ) w1
write( 6,8001 ) rufn(1), rufn(2)
write( 6,8024 ) fl
write( 6,8009 ) scheme
write( 6,8002 ) conk
write( 6,8003 ) a
write( 6,8007 ) fo
write( 6,8005 ) dtm, tcom, tmaxm

```

```

write( 6,8018 ) fspace
write( 6,8006 ) d, f
write( 6,8010 ) req
write( 6,8014 ) ipao
write( 6,8004 )
write( 6,8000 )
do 40 i = 1, nsurg
40 write( 6,8016 ) i, qin( i ), cytime( i )
write( 6,8022 )
write( 6,8023 )
do 50 i = 1, nsorchg
50 write( 6,8019 ) xsorchg(i), so(i)

```

c

c

```

temp1 = conk
ncell = max
temp2 = fo
dt = dtm*60.0
tmax = tmaxm*60.0
amp1 = f/2.0
amm1 = amp1 - 1.0
phi = 0.65
theta = 0.65
ifl = int( fl )
tb = ( fo/( a*conk )) ** ( 1.0/( a-1.0 ))
itemp = int( tb )
test = tb - real(itemp)
if (test .ge. 0.45) tbasic = real(itemp) + 1.0
if (test .lt. 0.45) tbasic = real(itemp)
write( 6,8017 ) tbasic
tbasic = tbasic*60.0
roff = 0.0
iflfiv = int( fl/5.0 )

```

c

c

c Set T2T(k) Array = 0.0, to Be Able to

c Run &gt; 1 Data Sets

c \*\*\*\*\*

c

```

do 60 k = 0, max
xt( k ) = 0.0
tdx( k ) = 0.0
dtzt( k ) = 0.0
60 tzt( k ) = 0.0
do 80 k = 0, 20
80 xtt( k ) = 0.0

```

c

c

```

do 5000 ijk = 1, nsurg
iii = 0
do 100 i = 0, ncell
opt( i ) = 0.0
optrat( i ) = 0.0

```

```

100  xapre( i ) = 0.0
    if ( ijk .eq. 1 ) go to 140
    do 120  ii = 0, ncell
        xapre( ii ) = xa( ii )
        opt( ii ) = tr( ii ) - ta( ii )
        optrat( ii ) = opt( ii )/( cytime( ijk-1 )*60. )
        if ( optrat( ii ) .gt. 1.0 ) optrat( ii ) = 1.0
120  if ( xapre( ii ) .lt. xtt( ijk-2 ) ) optrat( ii ) = 1.0
140  continue

c
c  *****
c      Begin Advance Calculations
c  *****
c
c  *****
c  Assign TCO, QIN, AO for Each Surge
c
c
c      tco = cytime(ijk) * 60.0
c      k = 1
c      call coeff ( k, alpha )
c      ao = ( qin(ijk) / alpha ) ** ( 1. / ampi )
c
c
c      do 160  k = 0, max
c          ap(k) = 0.0
c          an(k) = 0.0
c          zp(k) = 0.0
c          tr(k) = 0.0
c          zn(k) = 0.0
c          to(k) = 0.0
c          ta(k) = 0.0
c          xa(k) = 0.0
160  dx(k) = 0.0
c      j = 1
c      to(1) = dt
c      ncell = 1
c      kr = 0
c      ka = 1
c
c
c  *****
c  Compute Initial Advance Increment
c  *****
c
c
c      conk = temp1
c      fo = temp2
c      k = -1
c      if (scheme .eq. 'csu') then
c          call csuzn(k)
c      else
c          call scszn(k)
c      endif

```

```

c
c
200  dx( 1 ) = ( qin(ijk)*dt*theta )/( phi*( ao+zn(0) ) )
    ta( 1 ) = dt
    xa( 1 ) = dx( 1 )
    an( 0 ) = ao
    an( 1 ) = 0.0
    zn( 1 ) = 0.0
    tr( 0 ) = tco + dt
220  j = j + 1
    do 240 k = 0, ncell
        ap(k) = an(k)
240  zp(k) = zn(k)
    to(j) = float(j) * dt
    if ( to(j-1) .gt. tmax ) go to 700
    an(0) = ao

c
c          *****
c          Recession
c          *****
c
    if ( to( j ) .le. tco ) go to 320
    an(0) = 0.05*ao
    if ( tr(0) .ne. 0.0 ) an(0) = 0.0
260  if ( ap(kr+1) .gt. 0.05*ao ) go to 300
280  tr( kr+1 ) = to( j-1 )
    kr = kr + 1
    if ( kr .lt. ka ) go to 260
    go to 700
300  continue

c
c          *****
c          Calculate Infiltration for Each Cell
c          *****
c
320  do 580 k = 0, ncell
    if ( scheme.eq.'csu' ) then
        call csuzn (k)
    else
        call scszn (k)
    endif
580  continue
    if ( iii.eq.1 ) go to 700

c
c          *****
c          Compute Flow Profiles
c          *****
c
    do 620 k = 0, ka-1
    call coeff ( k, alpha )
    ql = alpha * an(k) ** amp1
    qj = alpha * ap(k) ** amp1

```

```

qm = alpha * ap(k+1) ** amp1
c2 = - ( theta*q1 + (1.-theta)*qj ) / theta / alpha
c2 = c2 + qm*(1.-theta) /alpha /theta
c2 = c2 + dx(k+1)*(phi*zn(k)+(1.-phi)*zn(k+1))/theta/dt/alpha
c2 = c2 - dx(k+1)*(phi*zp(k)+(1.-phi)*zp(k+1))/theta/dt/alpha
c2 = c2 + phi*dx(k+1)*an(k)/ theta/ dt/ alpha
c2 = c2 - dx(k+1)*(phi*ap(k)+(1.-phi)*ap(k+1))/theta/dt/alpha
c1 = dx(k+1) * (1.-phi)/dt/alpha/theta
i = 0

```

```

c
c *****
c Newton-Raphson Solution Procedure
c *****
c

```

```

        dan = 50.
        an(k+1) = 0.95*an(k)
600      i = i + 1
        if ( i.gt.50) print*,'cell--k=',k,' j=',j,' i=',i,' an(0)=',
c          an(0)
        if ( i.gt.50) print*,'an(k)=',an(k),' c1=',c1,' c2=',c2
        if ( i.gt.50) go to 700
        dak = (an(k+1)**amp1 + c1*an(k+1) + c2)/(amp1*an(k+1)**amm1 + c1)
        an(k+1) = an(k+1) - dak
        if ( an(k+1) .le. 0.0 ) an(k+1) = 0.0
        if ( abs( an(k+1)-dan ) .le. 0.00001 ) go to 620
        dan = an(k+1)
        go to 600
620      continue

c
c      if ( xa(ncell) .lt. fl ) go to 640
        call coeff ( k, alpha )
        roff = roff + ( alpha*( (1.-theta)*ap(ncell)**amp1 + theta*
c          an(ncell)**amp1) ) *dt
        go to 220
640      continue

c
c *****
c Compute Conditions for End Cell
c *****
c
c      n = ka + 1
        if ( an(ka).le.0.0 ) go to 680
        dx(n) = dt*theta*alpha*an(n-1)**amp1/((an(n-1)+zn(n-1))*phi)
        if ( dx(n) .le. 0.0 ) go to 220
        if ( ka .lt. ncell ) go to 660
        ncell = ncell + 1
        ta(n) = to(j)
        xa(n) = xa(n-1) + dx(n)
660      ka = ka + 1
        an(n) = 0.0
        zn(n) = 0.0
        go to 220

```

```

C
C *****
C      Front End Recession Computation
C *****
C
680      if ( an(ka).gt.0.0 ) go to 220
          tr(ka) = to(j)
          ka = ka - 1
          if ( ka.gt.kr ) go to 680

C
C *****
C      Print Results
C *****
C
C
700      continue
          if ( iii.eq.1 ) go to 740
          iii = 1
          do 720 k = 0, ncell
720      if ( zn(k).eq.0.0 ) go to 320
740      if ( ijk .ne. 1 ) call sursrt
          kb = ncell
          write ( 6,8015 )
          do 760 i = 0, ncell
              xt(i) = xa(i)
760      tdx(i) = dx(i)

C
C *****
C      Calculate Cumulative Times for Surges
C *****
C
          do 780 kk = 0, ncell
              t1(kk) = ta(kk)/60.0
              t2(kk) = tr(kk)/60.0
780      , tzt(kk) = tzt(kk) + zn(kk)
          do 800 kk = 0, ncell
800      write ( 6,8020 ) kk,xa(kk),t1(kk),t2(kk),zn(kk),tzt(kk)

C
C
          xtt(ijk) = xa(ncell)
          if ( xtt(ijk).le.xtt(ijk-1) .and. xtt(ijk).lt.fl ) go to 5500
          if ( xtt(ijk).ge.fl ) xtt(ijk) = fl

C
C
          if ( ijk.lt.nsurge ) go to 5000
          if ( infil.eq.1 ) go to 5000
          if ( xa(ncell) .ge. fl ) go to 820
          write ( 6,8050 )
820      do 840 ii = 0, max
              dtzt(ii) = 0.0
840      dist(ii) = 0.0
          call cinf5

```

```

      call eval
5000 continue
      go to 1
5500 write (6,8049)
8000 format( 1h ,10x,10hm**3/m/sec,2x,7hminutes,/)
8001 format(16h dry Manning n =, f6.4,17h, wet Manning n =, f6.4 )
8002 format( 3h k=,e10.4,14h m**3/m/min**a )
8003 format( 3h a=,e10.4 )
8004 format( 1h ,/,2x,5hnsurg,7x,3hqin,7x,6hcytime)
8005 format( 5h dtm=,e10.4,2h m,5h,cco=,e10.4,2h m,6h,tnax=,e10.4,1hm)
8006 format( 1h ,2hd=,f6.4,6h f=,f7.4,/)
8007 format(4h fo=,e10.4. /)
8008 format(a3)
8009 format(1h ,/, 23h infiltration scheme = , 3a)
8010 format(5h req=,f10.4)
8011 format(16a4)
8012 format(//1h ,16a4//)
8013 format(1h ,//,10x,30h***** UNIFORM FLOW MODEL ***** )
8014 format(6h ipao=,i4)
8015 format(1h ,//,6h node,7x,3h xa,10x,2hta,10x,2htr,8x,
      $      2h z,10x,2htz)
8016 format(1h ,i5,5x,f8.6,2x,f7.2)
8017 format(1h ,/,8h tbasic=,f8.0)
8018 format(1h ,/,8h fspace=, f8.5, 2h m)
8019 format(1h , 3x, f10.1, 2x, f8.6)
8020 format(1h ,i4,3f12.1,3e12.3)
8021 format(1h ,i4,e12.3)
8022 format(1h , /, 8x, 6hxsochg, 6x, 2hso)
8023 format(1h , 10x, 1hm, 7x, 3hm/m. /)
8024 format(1h , 4hfl =, e10.4, 2h m)
8049 format(1h ,//,12x,25hno further advance occurs)
8050 format(1h ,//,12x,24hend of field not reached)
      go to 1
      end

```

```

C
C *****
C
C      SUBROUTINE SRSRT
C
C *****
C
C      Subroutine to Accumulate Surge Flow Infiltration
C
C *****
C
      subroutine sursrt
      parameter ( max = 300 )
      common/a/ ncell, xt(0:max), kb, tdx(0:max)
      common/b/ xa(0:max), tzt(0:max)
      common/c/ dist(0:max), dt
      common/d/ iflfiv, dtzt(0:max), nsochg, d
      common/e/ nsurg, cytime(20), qin(20), req, roff, fl
      common/f/ to(0:max), ta(0:max), tr(0:max), opt(0:max)
      common/g/ xapre(0:max), xtt(0:20), xsochg(30), so(30)
      common/h/ rufn(2), fspace, iii, t, ijk, zn(0:max), j, ipao
      common/i/ conk, fo, a, optrat(0:max), tbasic, temp1, temp2
      dimension temp( 0:max )
      do 20 i = 0,max
20    temp(i) = 0.0
      i = 1
      do 100 k = 1,ncell
40    if ( xa(k).lt.xt(i)) go to 80
      if ( i.gt.kb ) go to 100
      if ( xa(k).eq.xt(i) .and. k.eq.ncell ) go to 60
      i = i+1
      go to 40
60    temp(k) = tzt( i)
      go to 100
80    temp(k) = tzt(i-1)+(tzt(i)-tzt(i-1))*(xa(k)-xt(i-1))/tdx(i)
100   continue
      do 120 i = 1,max
120   tzt(i) = temp(i)
      return
      end

```

```

C
C*****
C
C      SUBROUTINE CINF5
C
C*****
C
C      Subroutine CINF5 Calculates Tzt at 5 Meter Intervals
C      by Linear Interpolation After Initial Advance Is
C      Completed
C
C      Local Variables
C
C          DTZT = Infiltration at 5 Meter Spacings
C          DIST = 5 Meter Spacings From 0 to Field Length
C*****
C
      subroutine cinf5
      parameter ( max = 300 )
      common/a/ ncell, xt(0:max), kb, tdx(0:max)
      common/b/ xa(0:max), tzt(0:max)
      common/c/ dist(0:max), dt
      common/d/ iflfiv, dtzt(0:max), nsochg, d
      common/e/ nsurg, cytime(20), qin(20), req, roff, fl
      common/f/ to(0:max), ta(0:max), tr(0:max), opt(0:max)
      common/g/ xapre(0:max), xtt(0:20), xsochg(30), so(30)
      common/h/ rufn(2), fspace, iii, t, ijk, zn(0:max), j, ipao
      common/i/ conk, fo, a, optrat(0:max), tbasic, temp1, temp2
      dist(0) = 0.0
      dtzt(0) = tzt(0)
      do 60 kk = 1, iflfiv
          dist(kk) = dist(kk-1) + 5.0
          ii = 1
20      if ( xa(ii).ge.dist(kk) ) go to 40
          ii = ii + 1
          go to 20
40      dxa = (dist(kk)-xa(ii-1)) / (xa(ii)-xa(ii-1))
          dtzt(kk) = tzt(ii-1) + dxa*(tzt(ii)-tzt(ii-1))
          if (dtzt(kk).gt.1.) dtzt(kk) = 0.0
60 continue
      return
      end

```

```

C*****
C
C      SUBROUTINE EVAL
C
C*****
C
C      subroutine eval
C
C*****
C
C      Subroutine Eval Calculates Evaluation Parameters
C      and Water Volumes for an Irrigation
C
C      Local Variables
C
C      EA = Application Efficiency
C      ER = Requirement Efficiency (Storage Efficiency)
C      TWP = Tailwater Percentage
C      DPP = Deep Percolation Percentage
C      UCC = Christiansen's Uniformity Coefficient
C      VOLAP = Total Volume of Water Applied Over Field Length,
C              in Meters**3/Meter Width
C      VINFL = Total Volume Infiltrated for Field Length,
C              Calculated by the Trapezoidal Method,
C              in Meters**3/Meter Width
C      VREQ = Total Volume of Requirement for Field Length,
C              in Meters**3/Meter Width
C      VTW = Total Volume of Tailwater in Meters**3/Meter Width
C      VWSTO = Volume of Water Stored in Root Zone,
C              in Meters**3/Meter Width
C      YY = Temporary Summation of DTZT-YAVE in UCC Calculations
C      YTOT = Temporary Summation of DTZT in UCC Calculations
C      YAVE = Average DTZT in UCC Calculations
C      DISTN = Number of Points Evaluated in UCC Calculations
C      WSTO(II) = Array of Water Stored Values at 5 Meter Intervals
C
C*****
C
C      parameter ( max = 300 )
C      common/a/ ncell, xt(0:max), kb, tdx(0:max)
C      common/b/ xa(0:max), tzt(0:max)
C      common/c/ dist(0:max), dt
C      common/d/ iflfiv, dtzt(0:max), nsorch, d
C      common/e/ nsurg, cytime(20), qin(20), req, roff, fl
C      common/f/ to(0:max), ta(0:max), tr(0:max), opt(0:max)
C      common/g/ xapre(0:max), xtt(0:20), xsochg(30), so(30)
C      common/h/ rufn(2), fspace, iii, t, ijk, zn(0:max), j, ipao
C      common/i/ conk, fo, a, optrat(0:max), tbasic, temp1, temp2
C      dimension dp(0:max), wsto(0:max)
C
C      *****
C      Total Volume Applied
C      *****

```

```

C      volap = 0.0
      do 20 ii = 1,nsurg
20  volap = volap + cytime(ii)*qin(ii)*60.0
C
C      *****
C      Total Volume Infiltrated
C      *****
C
      vinf = 0.0
      do 40 ii = 1, ififiv
40  vinf = vinf + (dtzt(ii)-dtzt(ii-1))*0.5*5.0
C
C      *****
C      Total Volume of Deep Percolation
C      *****
C
      vdp = 0.0
      do 60 ii = 0,max
        wsto(ii) = 0.0
60  dp(ii) = 0.0
      do 80 ii = 0, ififiv
        dp(ii) = dtzt(ii) - req
        if (dp(ii).le.0.0) dp(ii) = 0.0
80  continue
      do 100 ii = 0, ififiv
100 vdp = vdp + (dp(ii)+dp(ii-1))*0.5*5.0
C
C      *****
C      Tailwater
C      *****
C
      vtw = 0.0
      vtw = roff
      if (vtw.lt.0.0) vtw = 0.0
C
C      ****
C      UCC
C      ****
C
      yy = 0.0
      ytot = 0.0
      yave = 0.0
      distn = 0.0
      ucc = 0.0
      do 120 ii = 0, ififiv
120  ytot = ytot + dtzt(ii)
      distn = (fi/5.0) + 1.0
      yave = ytot/distn
      do 140 ii = 1, ififiv
140  yy = yy + abs( dtzt(ii)-yave )
      ucc = 1.0 - yy/(distn*yave)
C

```

```

C *****
C Volume of Water Stored in Root Zone
C *****
C
vwsto = 0.0
do 160 ii = 0, iflfiv
  if ( dtzt(ii) .le. req ) then
    wsto(ii) = dtzt(ii)
  else
    wsto(ii) = req
  endif
160 continue
do 180 ii = 1, iflfiv
180 vwsto = vwsto + (wsto(ii)+wsto(ii-1))*0.5*5.0
C
C *****
C Evaluation Parameters
C *****
C
vreq = req*fl
ea = (vwsto/volap)*100.0
er = (vwsto/vreq)*100.0
twp = (vtw/volap)*100.0
dpp = (vdp/volap)*100.0
write (6,8023)
write (6,8024)
do 860 kk = 0, iflfiv
860 write (6,8022) dist(kk),dtzt(kk),dp(kk),wsto(kk)
write (6,8025) volap
write (6,8026) vinf
write (6,8030) vwsto
write (6,8027) vdp
write (6,8028) vtw
write (6,8029) ucc
write (6,8031) ea
write (6,8032) er
write (6,8033) twp
write (6,8034) dpp
8022 format(1h ,4f10.4)
8023 format(1h ,/,12x,23hcumulative infiltration)
8024 format(1h ,/,5x,4hdist,7x,4hdtzt,6x,2hdp,7x,4hwsto)
8025 format(/7h volap=,f10.4)
8026 format(6h vinf=,1x,f10.4)
8027 format(5h vdp=,2x,f10.4)
8028 format(5h vtw=,2x,f10.4)
8029 format(/5h ucc=,2x,f10.4)
8030 format(7h vwsto=,f10.4)
8031 format(4h ea=,3x,f10.4)
8032 format(4h er=,3x,f10.4)
8033 format(5h twp=,2x,f10.4)
8034 format(5h dpp=,2x,f10.4)
return
end

```

```

C*****
C
C SUBROUTINE CSUZN
C*****
C
C Dr. F.T. Izuno's Infiltration Subroutine
C Employs Clemmens Branch Infiltration
C Function.
C*****
C
C subroutine csuzn (k)
C parameter ( max = 300 )
C common/a/ ncell, xt(0:max), kb, tdx(0:max)
C common/b/ xa(0:max), tzt(0:max)
C common/c/ dist(0:max), dt
C common/d/ iflfiv, dtzt(0:max), nsochg, d
C common/e/ nsurg, cytime(20), qin(20), req, roff, fl
C common/f/ to(0:max), ta(0:max), tr(0:max), opt(0:max)
C common/g/ xapre(0:max), xtt(0:20), xsochg(30), so(30)
C common/h/ rufn(2), fspace, iii, t, ijk, zn(0:max), j, ipao
C common/i/ conk, fo, a, optrat(0:max), tbasic, temp1, temp2
C
C *****
C Calculating Infiltration for the Initial
C Advance Increment
C *****
C
C if ( ijk .eq. 1 .and. k .lt. 0 ) then
C     t = dt
C     k = 0
C     go to 560
C else if ( k .lt. 0 ) then
C     t = dt
C     k = 0
C     go to 460
C endif
C
C *****
C Calculation of the Opportunity Times
C *****
C
C if ( iii .eq. 1 ) go to 340
C t = to( j ) - ta( k )
C if ( to(j).ge.tr(k) .and. tr(k).ne.0.0 ) t = tr(k)-ta(k)
C if ( iii .eq. 0 ) go to 360
340 t = tr(k) - ta(k)
C
C 360 conk = temp1
C     fo = temp2
C
C *****

```

```

c      Determining if Surge Flow or Continuous Flow
c      Infiltration Is to be Modeled
c      *****
c
c      if ( nsurg .eq. 1 ) go to 540
c      if ( xa(k) .ge. xtt(ijk-1) .and. xtt(ijk-1) .lt. fl .and.
c          t .lt. tbasic ) go to 520
c      if ( xa(k) .ge. xtt(ijk-1) .and. xtt(ijk-1) .lt. fl .and.
c          t .ge. tbasic ) go to 500
c      if ( xtt(ijk-2) .ge. fl ) go to 460
c      if ( xa(k) .lt. xtt(ijk-2) ) go to 460
c      i = 0
380  if ( xa(k) .lt. xapre(i) ) go to 400
c      if ( xa(k) .eq. xapre(i) ) go to 420
c      if ( xa(k) .gt. xapre(i) .and. xapre(i) .ge. fl ) go to 460
c      i = i + 1
c      go to 380
c
c      *****
c      Calculation of the Opportunity Times
c      for the Transition Function
c      *****
c
c      400  opp = ( optrat(i) + optrat(i-1) ) / 2.0
c           go to 440
c      420  opp = optrat(i)
c      440  conk = temp1 - temp1*opp
c           fo = temp2*opp
c           go to 480
c      460  fo = temp2
c           conk = 0.0
c
c      *****
c      Calculation of the Volume of Infiltrated Water
c      *****
c
c      480  zn(k) = conk*( t/60. ) ** a + fo*( t/60. )
c           if ( ipao .eq. 2 .and. ijk.eq.nsurg .and. xtt(ijk-1).ge.
c               fl .and. zn(k).le.temp2*t/60. ) zn(k) = temp2*t/60.
c           go to 580
c      500  zn(k) = conk*(tbasic/60.)**a + temp2*((t-tbasic)/60.)
c           go to 580
c      520  zn(k) = conk*(t/60.)**a
c           go to 580
c      540  if ( t.le.tbasic ) go to 580
c           zn(k) = conk*(tbasic/60.)**a + temp2*(( t-tbasic )/60.)
c           go to 580
c      560  zn(k) = conk*( t/60. )**a
c      580  return
c           end

```

```

C*****
C
C   SUBROUTINE SCSZN
C
C*****
C
C   A Subroutine to Calculate the Infiltrated Volume
C   Using the Soil Conservation Service's Design
C   Infiltration Equation. Surge Flow Infiltration
C   is Simulated by Assuming that the Off-Time
C   Effect is Equal to the Previous On-Time
C
C*****
C
C   Local variables
C
C   CYPREV   Cumulative value of the previous on- and off-time, min
C   SCSFAC   SCSPER / furrow spacing
C   SCSPER   The adjusted wetted perimeter, m
C   SCSTEM   Temporary variable used in the calculation of the
C             adjusted wetted perimeter
C   ZNNEG    Infiltrated depth during the previous on- and off-times,
C             used in the modeling of surge flow infiltration, m
C   ZNPOS    Infiltrated depth during the present on-time plus the
C             previous on- and off-times, used during the modeling
C             of surge flow infiltration, m
C*****
C
C
C   subroutine scszn ( k )
C   parameter ( max = 300 )
C   common/a/ ncell, xt(0:max), kb, tdx(0:max)
C   common/b/ xa(0:max), tzt(0:max)
C   common/c/ dist(0:max), dt
C   common/d/ iflfiv, dtzt(0:max), nsochg, d
C   common/e/ nsurg, cytime(20), qin(20), req, roff, fl
C   common/f/ to(0:max), ta(0:max), tr(0:max), opt(0:max)
C   common/g/ xapre(0:max), xtt(0:20), xsochg(30), so(30)
C   common/h/ rufn(2), fspace, iii, t, ijk, zn(0:max), j, ipao
C   common/i/ conk, fo, a, optrat(0:max), tbasic, temp1, temp2
C
C*****
C   Calculating Infiltration for the Initial
C   Advance Increment
C*****
C
C   if (k .lt. 0) then
C     t = dt
C     k = 0
C     go to 200
C   endif
C   if ( iii .eq. 1 ) go to 100

```

```

t = to( j ) - ta( k )
if ( to(j).ge.tr(k) .and. tr(k).ne.0.0 ) t = tr(k)-ta(k)
if ( iil .eq. 0 ) go to 200
100  t = tr(k) - ta(k)
200  continue
    if ( t.lt.0 ) return
    i = 0

c
c *****
c Calculating the Opportunity Time for Sections
c During the Second Wetting
c *****
c
300  if ( xa(k).lt.xapre(i) ) then
    opp = (opt(i) + opt(i-1)) / 2.
    go to 400
    else if ( xa(k).eq.xapre(i) ) then
        opp = opt(i)
        go to 400
    else if ( xa(k).gt.xapre(i) .and. xapre(i).ge.fl ) then
        go to 400
    endif
    i = i + 1
    go to 300
400  continue
    jjj = 1
500  if ( xa(k).le.xsochg(jjj) ) go to 600
    jjj = jjj + 1
    go to 1585
600  continue
    znneg = 0.0
    znpos = 0.0
    cyprev = 0.0

c
c *****
c Calculations for the Shape Factor Asuming Variable
c Slope and Variable Surface-Roughness
c *****
c
    if ( xtt(ijk-1).gt.xa(k) ) then
        scstem = ( 1000.0*qin(ijk)*rufn(2) ) / ( so(jjj)**0.5 )
        scsper = ( 0.265 * (scstem) **0.425 ) + 0.227
        scsfac = scsper / fspace
    else
        scstem = ( 1000.0*qin(ijk)*rufn(1) ) / ( so(jjj)**0.5 )
        scsper = ( 0.265 * (scstem) **0.425 ) + 0.227
        scsfac = scsper / fspace
    endif

c
c *****
c Calculation of the Infiltrated Volume,
c Determines Whether Advance is Over a
c Previously Wetted or Dry Furrow Section

```

```

c *****
c
c      if ( ijk.eq.1 .or. xa(k).gt.xtt(ijk-1) ) then
c          zn(k) = ((conk*(t/60.0)**a + 7.) * scsfac) / 1000.0
c      else
c
c *****
c      Determining the Cumulative On- and Off-Times
c      for the Previous Surges
c *****
c
c      cyprev = 0.0
c      if ( xa(k).ge.xtt(ijk-2) .and. xa(k).lt.xtt(ijk-1) )then
c          cyprev = 2.0 * opp / 60.
c          if (cyprev.gt.2*cytime(ijk-1)) cyprev = 2*cytime(ijk-1)
c      else
700      ix = 0
c          if ( xtt(ix).ge.xa(k) ) go to 800
c          ix = ix + 1
c          go to 700
800      continue
c          do 900 ik = ix, ijk-1
c              cyprev = cyprev + 2.0*cytime(ik)
900      continue
c      endif
c      t = t + cyprev*60.0
c      znneg = ((conk*(cyprev**a) + 7.)*scsfac) / 1000.0
c      znpos = ((conk*(t/60.0)**a + 7.) * scsfac) / 1000.0
c      zn(k) = znpos - znneg
c      endif
c      return
c      end

```

```

C*****
C
C   SUBROUTINE COEFF
C*****
C
C   Subroutine COEFF Calculates the Value of the Coefficient
C   ALPHA. Determines if Advance Is Over a Previously Wetted
C   Furrow Section or a Dry Furrow Section. Also Determines
C   the Current Value of the Slope
C*****
C
      subroutine coeff ( k, alpha )
      parameter ( max = 300 )
      common/a/ ncell, xt(0:max), kb, tdx(0:max)
      common/b/ xa(0:max), tzt(0:max)
      common/c/ dist(0:max), dt
      common/d/ iflfiv, dtzt(0:max), nsochg, d
      common/e/ nsurg, cytime(20), qin(20), req, roff, fl
      common/f/ to(0:max), ta(0:max), tr(0:max), opt(0:max)
      common/g/ xapre(0:max), xtt(0:20), xsochg(30), so(30)
      common/h/ rufn(2), fspace, iii, t, ijk, zn(0:max), j, ipao
      common/i/ conk, fo, a, optrat(0:max), tbasic, temp1, temp2
      if ( xa(ncell) .ge. fl ) then
        alpha = sqrt( so(nsochg)*d ) / rufn(2)
      else
        1count = 1
C
C   *****
C   Determination of the Current Value of the Slope
C   *****
C
      100      if ( xa(k) .le. xsochg(1count) ) go to 200
              1count = 1count + 1
              go to 100
      200      continue
C
C   *****
C   Calculation of the value of ALPHA
C   *****
C
              if ( xtt(ijk-1) .gt. xa(k) ) then
                alpha = sqrt( so(1count)*d ) / rufn(2)
              else
                alpha = sqrt( so(1count)*d ) / rufn(1)
              endif
      endif
      return
      end

```

## SAMPLE INPUT FILE

## INPUT DATA FILE FORMAT

```

INPMOD
W1
RUFN(1) RUFN(2) EL
DTM
D F
FSPACE
TCOM TMAXM
NSURG
QIN(1) CYTIME(1)
.
.
.
NSOCHG
XSOCHG(1) S0(1)
.
.
.
SCHEME
FO CONK A
IPAO INFIL
REQ
INPMOD

```

## SAMPLE INPUT FILE

```

1
EXAMPLE SIMULATION
0.03 0.02 300.0
1
0.5627 2.884
0.7618
500. 500.
4
0.0024 30.
0.0024 30.
0.0024 30.
0.0024 30.
2
200. 0.004
350. 0.003
csu
0.00025 .004 .55
1 1
0.084
0

```

SAMPLE OUTPUT FILE

## \*\*\*\*\* UNIFORM FLOW MODEL \*\*\*\*\*

## EXAMPLE SIMULATION

dry Manning n =0.0300, wet Manning n =0.0200

fl =0.3000e+03 m

infiltration scheme = csu

k=0.4000e-02 m\*\*3/m/min\*\*a

a=0.5500e+00

fo=0.2500e-03

dtm=0.1000e+01 m,tco=0.5000e+03 m,tmax=0.5000e+03m

fspace= 0.76180 m

d=0.5627 f= 2.8840

req= 0.0840

ipao= 1

nsurg	qin m**3/m/sec	cytime minutes
1	0.002400	30.00
2	0.002400	30.00
3	0.002400	30.00
4	0.002400	30.00

xsochg m	so m/m
200.0	0.004000
350.0	0.003000

tbasic= 126.

node	xa	ta	tr	z	tz
0	0.0	0.0	31.0	0.264e-01	0.264e-01
1	9.5	1.0	32.0	0.264e-01	0.264e-01
2	18.6	2.0	33.0	0.264e-01	0.264e-01
3	27.2	3.0	34.0	0.264e-01	0.264e-01
4	35.2	4.0	35.0	0.264e-01	0.264e-01
5	42.8	5.0	36.0	0.264e-01	0.264e-01
6	49.9	6.0	37.0	0.264e-01	0.264e-01
7	56.6	7.0	38.0	0.264e-01	0.264e-01
8	62.9	8.0	39.0	0.264e-01	0.264e-01
9	68.9	9.0	40.0	0.264e-01	0.264e-01
10	74.6	10.0	41.0	0.264e-01	0.264e-01
11	80.2	11.0	42.0	0.264e-01	0.264e-01
12	85.4	12.0	42.0	0.260e-01	0.260e-01

13	90.5	13.0	42.0	0.255e-01	0.255e-01
14	95.4	14.0	42.0	0.250e-01	0.250e-01
15	100.2	15.0	42.0	0.245e-01	0.245e-01
16	104.7	16.0	43.0	0.245e-01	0.245e-01
17	109.2	17.0	43.0	0.240e-01	0.240e-01
18	113.5	18.0	43.0	0.235e-01	0.235e-01
19	117.7	19.0	43.0	0.230e-01	0.230e-01
20	121.8	20.0	43.0	0.224e-01	0.224e-01
21	125.7	21.0	44.0	0.224e-01	0.224e-01
22	129.6	22.0	44.0	0.219e-01	0.219e-01
23	133.4	23.0	44.0	0.213e-01	0.213e-01
24	137.1	24.0	44.0	0.208e-01	0.208e-01
25	140.7	25.0	44.0	0.202e-01	0.202e-01
26	144.2	26.0	44.0	0.196e-01	0.196e-01
27	147.7	27.0	45.0	0.196e-01	0.196e-01
28	151.1	28.0	45.0	0.190e-01	0.190e-01
29	154.5	29.0	45.0	0.184e-01	0.184e-01
30	157.7	30.0	45.0	0.177e-01	0.177e-01
31	160.9	31.0	45.0	0.171e-01	0.171e-01
32	164.1	32.0	45.0	0.164e-01	0.164e-01
33	167.2	33.0	45.0	0.157e-01	0.157e-01
34	170.3	34.0	45.0	0.150e-01	0.150e-01
35	173.3	35.0	45.0	0.142e-01	0.142e-01
36	176.2	36.0	45.0	0.134e-01	0.134e-01
37	179.1	37.0	45.0	0.126e-01	0.126e-01
38	181.9	38.0	45.0	0.117e-01	0.117e-01
39	184.5	39.0	45.0	0.107e-01	0.107e-01
40	186.8	40.0	45.0	0.989e-02	0.969e-02
41	188.7	41.0	45.0	0.857e-02	0.857e-02
42	190.0	42.0	45.0	0.732e-02	0.732e-02
43	190.6	43.0	44.0	0.400e-02	0.400e-02

node	xa	ta	tr	z	tz
0	0.0	0.0	31.0	0.775e-02	0.342e-01
1	16.7	1.0	32.0	0.775e-02	0.342e-01
2	33.3	2.0	33.0	0.775e-02	0.342e-01
3	49.7	3.0	34.0	0.775e-02	0.342e-01
4	66.0	4.0	35.0	0.775e-02	0.342e-01
5	82.2	5.0	36.0	0.775e-02	0.340e-01
6	98.2	8.0	37.0	0.931e-02	0.340e-01
7	113.3	7.0	38.0	0.106e-01	0.341e-01
8	127.7	8.0	39.0	0.124e-01	0.346e-01
9	141.0	9.0	40.0	0.149e-01	0.351e-01
10	153.0	10.0	41.0	0.162e-01	0.348e-01
11	164.1	11.0	42.0	0.180e-01	0.344e-01
12	174.1	12.0	43.0	0.205e-01	0.345e-01
13	182.8	13.0	44.0	0.224e-01	0.337e-01
14	190.4	14.0	45.0	0.252e-01	0.303e-01
15	196.9	15.0	46.0	0.264e-01	0.264e-01
16	202.6	16.0	47.0	0.264e-01	0.264e-01
17	205.3	17.0	47.0	0.260e-01	0.260e-01
18	207.7	18.0	47.0	0.255e-01	0.255e-01

19	210.3	19.0	47.0	0.250e-01	0.250e-01
20	212.8	20.0	48.0	0.250e-01	0.250e-01
21	215.2	21.0	48.0	0.245e-01	0.245e-01
22	217.5	22.0	48.0	0.240e-01	0.240e-01
23	219.7	23.0	48.0	0.235e-01	0.235e-01
24	221.8	24.0	48.0	0.230e-01	0.230e-01
25	223.8	25.0	48.0	0.224e-01	0.224e-01
26	225.7	26.0	48.0	0.219e-01	0.219e-01
27	227.6	27.0	48.0	0.213e-01	0.213e-01
28	229.5	28.0	48.0	0.208e-01	0.208e-01
29	231.2	29.0	49.0	0.208e-01	0.208e-01
30	233.0	30.0	49.0	0.202e-01	0.202e-01
31	234.6	31.0	49.0	0.196e-01	0.196e-01
32	236.3	32.0	49.0	0.190e-01	0.190e-01
33	237.9	33.0	49.0	0.184e-01	0.184e-01
34	239.4	34.0	49.0	0.177e-01	0.177e-01
35	241.0	35.0	49.0	0.171e-01	0.171e-01
36	242.5	36.0	49.0	0.164e-01	0.164e-01
37	243.9	37.0	49.0	0.157e-01	0.157e-01
38	245.3	38.0	49.0	0.150e-01	0.150e-01
39	246.7	39.0	49.0	0.142e-01	0.142e-01
40	248.1	40.0	49.0	0.134e-01	0.134e-01
41	249.4	41.0	49.0	0.126e-01	0.126e-01
42	250.7	42.0	49.0	0.117e-01	0.117e-01
43	251.8	43.0	48.0	0.969e-02	0.969e-02
44	252.7	44.0	48.0	0.857e-02	0.857e-02
45	253.4	45.0	48.0	0.732e-02	0.732e-02
46	253.8	46.0	47.0	0.400e-02	0.400e-02

node	xa	ta	tr	z	tz
0	0.0	0.0	31.0	0.775e-02	0.419e-01
1	16.7	1.0	32.0	0.775e-02	0.419e-01
2	33.3	2.0	33.0	0.775e-02	0.419e-01
3	49.7	3.0	34.0	0.775e-02	0.419e-01
4	66.0	4.0	35.0	0.775e-02	0.419e-01
5	82.2	5.0	36.0	0.775e-02	0.418e-01
6	98.2	6.0	37.0	0.775e-02	0.418e-01
7	114.0	7.0	38.0	0.775e-02	0.418e-01
8	129.7	8.0	39.0	0.775e-02	0.424e-01
9	145.2	9.0	40.0	0.775e-02	0.427e-01
10	160.5	10.0	41.0	0.775e-02	0.423e-01
11	175.6	11.0	42.0	0.775e-02	0.421e-01
12	190.5	12.0	43.0	0.775e-02	0.380e-01
13	205.3	13.0	45.0	0.832e-02	0.343e-01
14	219.7	14.0	46.0	0.115e-01	0.349e-01
15	230.4	15.0	46.0	0.140e-01	0.348e-01
16	240.0	16.0	47.0	0.174e-01	0.349e-01
17	248.1	17.0	48.0	0.205e-01	0.339e-01
18	255.0	18.0	49.0	0.264e-01	0.264e-01
19	260.3	19.0	50.0	0.264e-01	0.264e-01
20	262.7	20.0	51.0	0.264e-01	0.264e-01
21	265.4	21.0	51.0	0.260e-01	0.260e-01

22	268.0	22.0	51.0	0.255e-01	0.255e-01
23	270.4	23.0	51.0	0.250e-01	0.250e-01
24	272.7	24.0	51.0	0.245e-01	0.245e-01
25	274.8	25.0	52.0	0.245e-01	0.245e-01
26	276.8	26.0	52.0	0.240e-01	0.240e-01
27	278.7	27.0	52.0	0.235e-01	0.235e-01
28	280.5	28.0	52.0	0.230e-01	0.230e-01
29	282.2	29.0	52.0	0.224e-01	0.224e-01
30	283.8	30.0	52.0	0.219e-01	0.219e-01
31	285.4	31.0	52.0	0.213e-01	0.213e-01
32	287.0	32.0	52.0	0.208e-01	0.208e-01
33	288.5	33.0	52.0	0.202e-01	0.202e-01
34	289.9	34.0	52.0	0.196e-01	0.196e-01
35	291.3	35.0	52.0	0.190e-01	0.190e-01
36	292.7	36.0	52.0	0.184e-01	0.184e-01
37	294.0	37.0	52.0	0.177e-01	0.177e-01
38	295.3	38.0	53.0	0.177e-01	0.177e-01
39	296.6	39.0	53.0	0.171e-01	0.171e-01
40	297.8	40.0	53.0	0.164e-01	0.164e-01
41	299.0	41.0	53.0	0.157e-01	0.157e-01
42	300.2	42.0	53.0	0.150e-01	0.150e-01

node	xa	ta	tr	z	tz
0	0.0	0.0	31.0	0.775e-02	0.497e-01
1	15.1	1.0	32.0	0.775e-02	0.497e-01
2	32.9	2.0	34.0	0.800e-02	0.499e-01
3	50.4	3.0	35.0	0.800e-02	0.499e-01
4	67.7	4.0	36.0	0.800e-02	0.499e-01
5	84.8	5.0	37.0	0.800e-02	0.498e-01
6	101.7	6.0	38.0	0.800e-02	0.498e-01
7	118.4	7.0	39.0	0.800e-02	0.500e-01
8	135.0	8.0	39.0	0.775e-02	0.503e-01
9	151.3	9.0	41.0	0.800e-02	0.506e-01
10	167.5	10.0	41.0	0.775e-02	0.500e-01
11	183.6	11.0	42.0	0.775e-02	0.477e-01
12	199.4	12.0	43.0	0.775e-02	0.435e-01
13	215.1	13.0	44.0	0.775e-02	0.425e-01
14	230.6	14.0	45.0	0.775e-02	0.425e-01
15	243.6	15.0	46.0	0.775e-02	0.422e-01
16	256.5	16.0	47.0	0.775e-02	0.342e-01
17	269.4	17.0	48.0	0.868e-02	0.339e-01
18	281.7	18.0	49.0	0.118e-01	0.344e-01
19	292.6	19.0	50.0	0.162e-01	0.346e-01
20	301.8	20.0	51.0	0.775e-02	0.775e-02

OPTIMIZATION OF SURGE IRRIGATION

by

Terry William Ortel

B.S., Purdue University; 1984

---

AN ABSTRACT OF A MASTER'S THESIS

submitted in partial fulfillment of the

requirements for the degree

MASTER OF SCIENCE

in

AGRICULTURAL ENGINEERING

Department of Agricultural Engineering

Kansas State University  
Manhattan, Kansas

1986

## ABSTRACT

The objectives of this study were to expand a kinematic-wave model to simulate the effects of a variable slope profile and variable degrees of surface-roughness, to incorporate the Soil Conservation Service's design infiltration equation into the kinematic-wave model and to optimize, by computer simulation, the surge irrigation strategy for selected soils in western Kansas.

During the 1985 irrigation season, field tests were conducted on three sites in western Kansas. At one of these locations, a pronounced break in the field slope existed. Pre-irrigation, first irrigation, and second irrigation tests were conducted using both surge and continuous flows.

Simulation studies involving the variable slope and variable surface-roughness subroutine were found to accurately model the advance of irrigation water. The variable slope and variable surface-roughness subroutine was shown to reduce the magnitude of the relative error in the resulting advance distance when compared to a model with an assumed average slope and surface-roughness.

The kinematic-wave model can accurately simulate the test row for which the intake coefficients were fit; however, upon using these coefficients and varying the surge-flow on-times, it was found that the predicted advance rates did not coincide with those observed in the field. Hence, advance-rate trends that were observed in the field could not be reproduced by the model.

The Soil Conservation Service's design infiltration equation, using the Intake Family tabulated coefficients, was found to be too general to be

applied for modeling purposes. Because the kinematic-wave model is sensitive to the intake rate coefficients, the SCS's method of grouping various soil types under one intake family is not specific enough for simulation applications.

Prior to optimizing the surge-flow irrigation strategy, values of the intake coefficients must be found for the soil conditions under consideration. The current version of the kinematic-wave model can provide estimates of the time for advance completion; however, the model was found to be specific for both the irrigation event and soil type. Similar soil types were found to have varying intake coefficients depending on the irrigation event, inflow rate, and degree of soil compaction.